

NASA CONTRACTOR
REPORT

NASA CR- 123494-04-1

COMPUTER SIMULATION OF IMPURITY DIFFUSION IN SILICON

By J. D. Gassaway and J. A. Etheridge

Department of Electrical Engineering
Mississippi State University
State College, MS 39762

Interim Report, Part I

January 12, 1972

Prepared for

GEORGE C. MARSHALL SPACE FLIGHT CENTER
Marshall Space Flight Center, Alabama 35812

1. REPORT NO. NASA CR-123494		2. GOVERNMENT ACCESSION NO.		3. RECIPIENT'S CATALOG NO.	
4. TITLE AND SUBTITLE Computer Simulation of Impurity Diffusion in Silicon				5. REPORT DATE January 12, 1972	
				6. PERFORMING ORGANIZATION CODE	
7. AUTHOR(S) J. D. Gassaway and J. A. Etheridge				8. PERFORMING ORGANIZATION REPORT #	
9. PERFORMING ORGANIZATION NAME AND ADDRESS Department of Electrical Engineering Mississippi State University State College, Mississippi 39762				10. WORK UNIT NO.	
				11. CONTRACT OR GRANT NO. NAS8-26749	
				13. TYPE OF REPORT & PERIOD COVERED Contractor Report	
12. SPONSORING AGENCY NAME AND ADDRESS National Aeronautics and Space Administration George C. Marshall Space Flight Center, Alabama 35812				14. SPONSORING AGENCY CODE EC45	
15. SUPPLEMENTARY NOTES Electronics Development Division, Electronics and Control Laboratory					
16. ABSTRACT This part of the report for work carried out under contract NAS8-26749 deals with the Computer Simulation of Impurity Diffusion in Silicon. The importance of impurity diffusion techniques for constructing semiconductor devices is well known, and a computer model for simulating diffusion techniques is very desirable because data useful for design or analysis can be generated much more rapidly with greater economy and less tedium than when obtaining the data experimentally. The following report is divided into five sections followed by five appendices. In section 1 the elementary classical models for idealized diffusion conditions are discussed, because the ideas developed are subsequently used in the more realistic models discussed in Section 2. These more practical models do not generally allow analytic solutions but require some type of numerical analysis. The numerical techniques which are used are outlined in Section 3 with more details concerning implementation given in Appendices I and II. Section 4 gives some of the results which have been obtained with the computer programs implementing the numerical techniques with the programs given in Appendices III and IV. Section 5 deals with the special problems of impurity-rich interlayers forming between an oxide and silicon. Appendix V gives a set of computed curves for sheet resistance, junction depth, and oxide thickness for different diffusion schedules.					
17. KEY WORDS			18. DISTRIBUTION STATEMENT Unclassified-Unlimited COR: <i>Ben R. Hollis</i> EC01 <i>J. B. Moore</i> Director, E&C Lab		
19. SECURITY CLASSIF. (of this report) Unclassified		20. SECURITY CLASSIF. (of this page) Unclassified		21. NO. OF PAGES 83	22. PRICE NTIS

PREFACE

The importance of impurity diffusion techniques for constructing semi-conductor devices is well known, and a computer model for simulating diffusion techniques is very desirable because data useful for design or analysis can be generated much more rapidly with greater economy and less tedium than when obtaining the data experimentally.

This report consists of five sections and five appendices. In Section 1, the elementary classical models for idealized diffusion conditions are discussed, because the ideas developed are subsequently used in the more realistic models discussed in Section 2. These more practical models do not generally allow analytic solutions, but require some type of numerical analysis. The numerical techniques which are used are outlined in Section 3 with more details concerning implementation given in Appendices I and II. Section 4 gives some of the results which have been obtained with the computer programs implementing the numerical techniques with the programs given in Appendices III and IV. Section 5 deals with the special problems of impurity-rich interlayers forming between an oxide and silicon. Appendix V gives a set of computed curves for sheet resistance, junction depth, and oxide thickness for different diffusion schedules.

TABLE OF CONTENTS

	Page
LIST OF FIGURES	iv
LIST OF TABLES	v
 SECTIONS	
1. Idealized Diffusion Models	1
2. Practical Diffusion Models	6
3. Computational Methods	16
4. Results	21
5. Predeposition Diffusions	29
 APPENDICES	
I Normalization and Explicit Difference Method ...	I.1
II Implicit Difference Method	II.1
III Implicit Program Listing	III.1
IV Explicit Program Listing	IV.1
V Junction Depth, Sheet Resistance, and Oxide Thickness Curves	V.1

LIST OF FIGURES

Figure	Page
(2-1) The Temperature Dependence of B	7
(2-2) The Temperature Dependence of B/A	7
(2-3a) The Effect of a Growing Oxide on a Boron Impurity Profile	8
(2-3b) The Effect of a Growing Oxide on a Boron Impurity Profile	8
(4-1) Comparison of Predicted Results with the Results of Grove	23
(4-2) Comparison of Predicted Results with the Results of Kato and Nishi	24
(4-3) The Effect of the Electric Field on a Predeposition	25
(4-4) The Effect of the Electric Field as a Function of Temperature	26
(4-5) Profile Evolution for Phosphorus in an Oxidizing Ambient	28
(4-6) Profile Evolution for Boron in an Oxidizing Ambient	28
(5-1) Sheet Resistance vs. Time for Drive-In Diffusions in Nitrogen at 1150° with Boron- Rich Surface Layer	31
(5-2) Sheet Resistance and Junction-Depth vs. Time for B ₂ H ₆ , Diborane, Predeposition Diffusion	34

LIST OF TABLES

Table		Page
(4-1)	Some Predicted and Experimental Results for Several Ambient Changes	27

1. IDEALIZED DIFFUSION MODELS

Many of the practical techniques for diffusion, such as used for the fabrication of source and drain regions for the MOST, utilize a two-step diffusion process. The two-step process involves a predeposition step and a drive-in step which are described in this and the following sections. Practical diffusion schedules require a complex model description; however, the more complex practical model utilizes simpler concepts which are used to describe idealized diffusion conditions. In this section the equations used to describe idealized diffusion conditions are given.

Diffusion processes are usually described by Fick's first and second laws of diffusion.¹ Fick's first law defines a parameter called the diffusion constant or the diffusivity. In a one-dimensional model, it is described by

$$F = -D \frac{\partial N}{\partial x} \quad (1-1)$$

where F is the fluxdensity of particles, N is the concentration of impurity atoms (per cm^3), and D is the diffusion coefficient (cm^2/sec). This mathematical statement implies that the flux of particles is proportional to the gradient of the concentration. Particles move from denser to less dense regions. The negative

sign indicates that diffusion occurs from regions of high concentration to those of lower concentration.

The requirement that particles be conserved gives Fick's second law. In one dimension it is

$$\frac{\partial N}{\partial t} = - \frac{\partial F}{\partial x} \quad (1-2a)$$

Substituting equation (1-1) into (1-2a) gives;

$$\frac{\partial N}{\partial t} = \frac{\partial}{\partial x} \left[D \frac{\partial N}{\partial x} \right] \quad (1-2b)$$

The diffusion coefficient is assumed to be constant and equation (1-2) becomes

$$\frac{\partial N}{\partial t} = D \frac{\partial^2 N}{\partial x^2} \quad (1-3)$$

Solutions to equation (1-3) are usually used to describe diffusions. The solutions are of two general classes, those in which the impurities are externally added to the semiconductor and those in which impurities that have previously been deposited in the semiconductor are allowed to diffuse farther from the surface.

The first class of solutions are for diffusions called pre-depositions. A large concentration of impurities are diffused slightly beneath the surface of a semiconductor wafer. There is a heavy concentration of impurities in the ambient surrounding the wafer, and it is assumed that the surface concentration remains at a constant value equal to the solubility limit of the impurity in the semiconductor.

For boron in silicon the solubility limit is about $4.0 \times 10^{20} \text{ cm}^{-3}$.

For this type of diffusion the boundary conditions and initial conditions are

$$\begin{aligned} N(0, t) &= N_0 \\ N(\infty, t) &= 0 \\ N(x, 0) &= 0 \quad x \geq 0 \end{aligned} \quad (1-4)$$

where N_0 is the solubility limit.

The solution to (1-3) is then²

$$N(x, t) = N_0 \operatorname{ERFC}\left(\frac{x}{2\sqrt{Dt}}\right) \quad (1-5a)$$

where

$$\operatorname{ERFC}(y) = 1 - \frac{2}{\sqrt{\pi}} \int_0^y \exp(-u^2) du. \quad (1-5b)$$

The second class of solutions are for drive-in diffusions. The drive-in is performed after a predeposition in order to increase the penetration depth and decrease the surface concentration. In order to get a solution for the impurity profile after drive-in, the profile after the predeposition is approximated by

$$N(x, 0) = \begin{cases} N_0, & x \leq h \\ 0, & x > h \end{cases} \quad (1-6)$$

where $N_0 h = Q$ is the total number of impurities in the semiconductor after the predeposition.

$$Q = N_0 \int_0^{\infty} \operatorname{ERFC}(u) du \quad (1-7)$$

It is also assumed that the surface is impenetrable so that the flux of particles at the surface is zero.

$$D \frac{\partial N}{\partial x} \Big|_{x=0} = 0 \quad (1-8)$$

The second boundary condition requires that the concentration of impurities goes to zero as x approaches infinity. The semiconductor crystal is assumed to be infinite in the positive x direction. This can be assumed if the diffusion length, $2\sqrt{Dt}$, is small compared to the crystal thickness.

The solution to equation (1-3) for the drive-in condition can be approximated by equation (1-9).³

$$N(x, t) = \frac{Q}{\sqrt{Dt\pi}} \exp\left(-\frac{x^2}{4Dt}\right) \quad (1-9)$$

P-N junctions are formed by diffusing into a wafer that has a doping level that is opposite in polarity to the diffusing atoms. (Any process for introducing impurities into a semiconductor to produce some electrical property is called "doping".) The initial doping level is called the background doping. By definition, the junction is formed where the diffusing impurity concentration equals the background doping. The junction depth for the impurity profile in equation (1-9) is

$$x_j = \left(4Dt \ln \frac{Q}{N_b \sqrt{Dt\pi}}\right)^{1/2} \quad (1-10)$$

The junction depth is important in bipolar transistors because of its effect on the base width. For the double diffused transistor, the base width is the difference between the junction depth of the base diffusion and the junction depth of the emitter diffusion. The

injection efficiency, base resistance, current gain, and other parameters of the transistor depend on the base width. Since the base width is usually small, the junction depths must be controlled accurately.

Another important parameter is the sheet resistance defined by equation (1-11) for an "N-type", or donor impurity, diffusion.

$$\frac{1}{R_s} = \int_0^{x_j} q\mu_n n \, dx \quad (1-11)$$

In equation (1-11), R_s is the sheet resistance, q is the electronic charge, μ_n is the mobility of electrons, and n is the number of electrons. Practically, n can be taken to be the same as N , the impurity concentration, in many cases. The base spreading resistance in bipolar transistors, parasitic resistances in M-O-S transistors, and all parameters which depend on the impurity profile depend on the sheet resistance. It is also important to the process engineer since it can be measured easily and is an aid in determining some characteristics of the impurity profile.

2. PRACTICAL DIFFUSION MODELS

In this section some of the practical conditions for diffusion processes are considered. One of the first major deviations from the idealized diffusion process which must be considered is the effect of oxidation during a drive-in diffusion. The oxide is subsequently selectively etched to expose other areas to be diffused, or to expose areas that are to be electrically connected to an input or output of a device. The oxide that is not etched away is used for insulation, and, in some field effect devices, as part of the device itself.

The rate at which the oxide grows on the surface of the silicon depends on the temperature, the amount of oxide present, and on whether it is grown in a stream or oxygen ambient. The growth rate of the oxide is given by equation (2-1).⁴

$$\frac{dx_0}{dt} = \frac{B}{A + 2 \cdot x_0} \quad (2-1)$$

In this equation x_0 is the oxide thickness, and B and A are the parameters plotted as functions of temperature in Figure (2-1) and (2-2) respectively. The parameter B is called the parabolic rate constant, and B/A is called the linear rate constant.

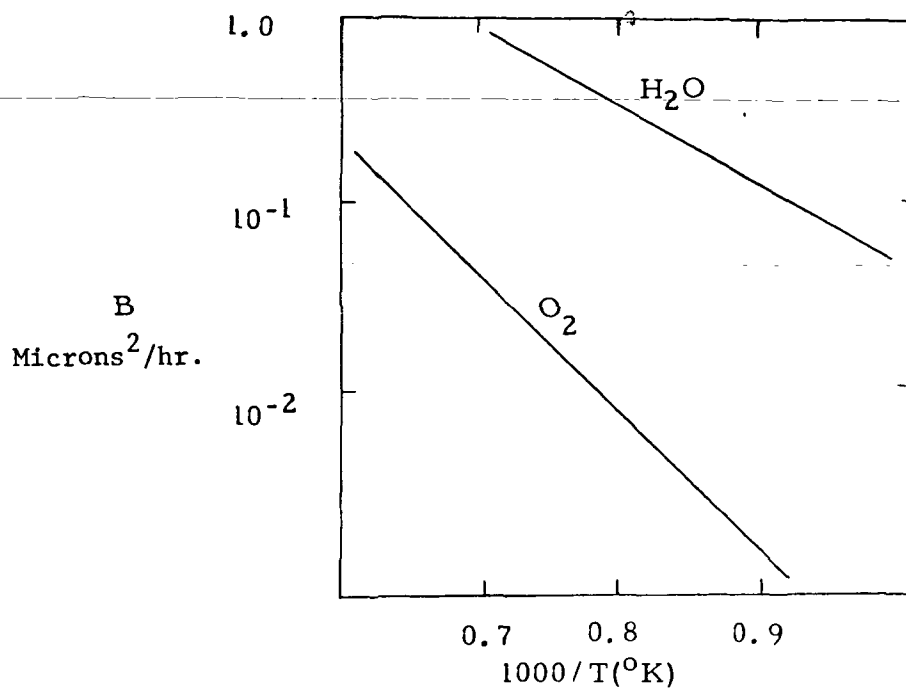


Figure (2-1). The Temperature Dependence of B .

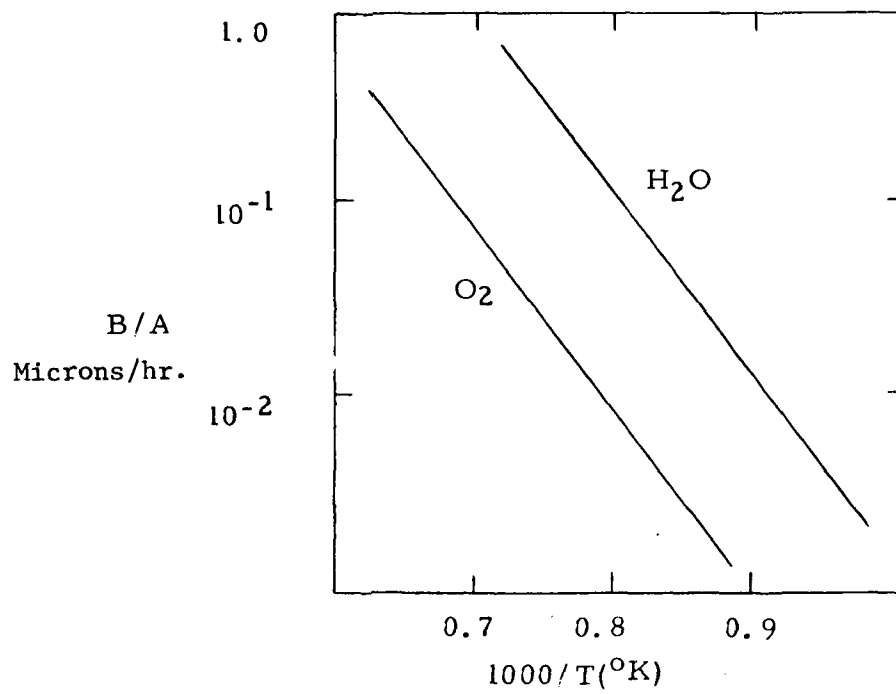


Figure (2-2). The Temperature Dependence of B/A .

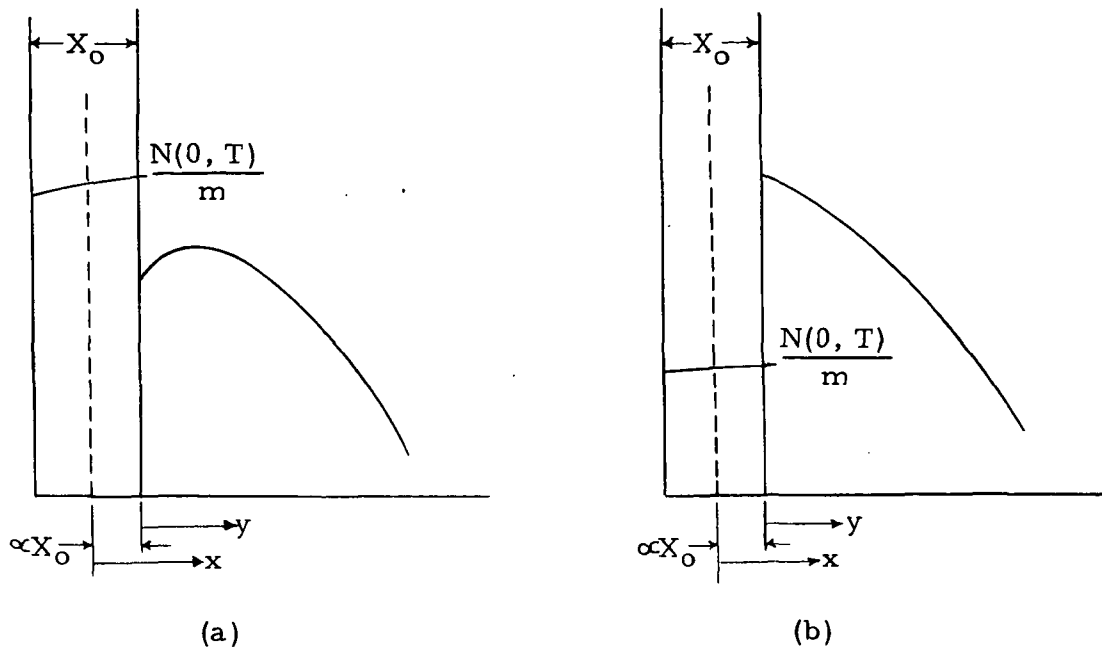


Figure (2-3). The Effect of a Growing Oxide on (a) a Boron Impurity Profile (b) a Phosphorus Impurity Profile.

After a wafer has been through the predeposition process, the oxide which is grown during the drive-in ideally masks the wafer so that the predeposited impurities cannot diffuse back out through the oxide. There will be some impurity concentration in the oxide, however, because of the segregation effect at the silicon-silicon dioxide interface. The effect of the growing oxide on a boron and a phosphorus diffusion are shown in Figure (2-3).⁵ A constant called the segregation coefficient relates the concentrations on the two sides of the interface. The segregation coefficient is defined by equation (2-2).

$$m = \frac{\text{Equilibrium concentration in the silicon}}{\text{Equilibrium concentration in the oxide}} \quad (2-2)$$

The segregation coefficient of boron is about 0.3, and for phosphorus it is about 10.0. From Figure (2-3) it can be seen that many of the boron atoms are lost to the oxide causing a depletion of impurities near the surface. For phosphorus a small amount of the impurity is lost to oxide, so that, as the oxide grows inward, it pushes the impurities in front of it. This in turn causes the concentration near the surface to remain at a higher value than is predicted by equation (1-9).

As the oxide grows, it consumes part of the wafer. The ratio of the thickness of the silicon consumed to the total oxide thickness is a constant called α , which accounts for the difference in the densities of the silicon and the oxide. The numerical value of α is approximately 0.45.⁶

With a growing oxide on the surface of the wafer, two deviations from the previous model for drive-in diffusion are immediately apparent. There is no longer a convenient stationary coordinate system. The surface is moving with a velocity of 0.45 times the growth rate of the oxide. Furthermore, because of the escape of impurities through the surface, the impurity gradient at the surface is not necessarily zero.

The surface boundary condition is derived by assuming that the oxide grows only at the silicon-silicon dioxide boundary, and by requiring that particles crossing the boundary are conserved. It is useful to redefine the spatial coordinate so that the moving boundary

is the new reference, $y=0$. This is done by the linear transformation

$$y = x - \alpha X_o. \quad (2-3)$$

Then a particle which is stationary in the x -coordinate system at a point corresponding to $y>0$ will have an instantaneous velocity due to the movement of the origin which is given by equation (2-4).

$$\frac{dy}{dt} = -\alpha \frac{dX_o}{dt} \quad (2-4)$$

Therefore there is an instantaneous flux of particles because of the moving boundary which is

$$F_1 = -\alpha \frac{dX_o}{dt} N(y, t), \quad y \geq 0. \quad (2-5)$$

From equation (1-1), the flux due to the impurity gradient is

$$F_2 = -D \frac{\partial N}{\partial y}. \quad (2-6)$$

The total instantaneous flux of particles in the semiconductor is the sum of the terms in equation (2-5) and (2-6).

With the assumption that all oxide growth takes place at the boundary, a particle inside the oxide has an instantaneous velocity due to oxide growth that is equal to the magnitude of the growth rate of the oxide. The velocity is in the negative y direction so the flux is the negative of the growth rate. Using the symbol C for the impurity concentration in the oxide, and D_o for the diffusion coefficient the total flux in the oxide is

$$F_o = -D_o \frac{\partial C}{\partial y} - \frac{dX_o}{dt} C(y, t). \quad (2-7)$$

Conservation of impurities at the boundary requires that the flux of particles at $y=0^-$ be equal to the flux at $y=0^+$. Equating the flux in the oxide and the flux in the semiconductor at the boundary gives

$$D \frac{\partial N}{\partial y} \Big|_{y=0^+} - D_o \frac{\partial C}{\partial y} \Big|_{y=0^-} = (K - \alpha) \frac{dX_o}{dt} N(0, t) \quad (2-8)$$

where $C(0, t)$ is replaced by $KN(0, t)$ on the right-hand side of equation (2-8), and K is the reciprocal of the segregation coefficient.

For impurities which diffuse slowly in the oxide, equation (2-8) reduces to

$$D \frac{\partial N}{\partial y} \Big|_{y=0} = (K - \alpha) \frac{dX_o}{dt} N(0, t). \quad (2-9)$$

For some impurities, such as boron and phosphorous, the diffusion in the oxide will be negligible.

The diffusion equation is written in terms of the new coordinate by returning to Fick's second law, equation (1-2a). By substituting the total flux of particles in the wafer into equation (1-2a), the new equation is

$$\frac{\partial N}{\partial t} = D \frac{\partial^2 N}{\partial y^2} + \alpha \frac{dX_o}{dt} \cdot \frac{\partial N}{\partial y}. \quad (2-10)$$

Equation (2-10) accounts for the oxide growth during the drive-in diffusion with the surface boundary condition of equation (2-9). For diffusion with an external source of impurities in an oxidizing atmosphere, the boundary condition would not be the same.

The diffusing impurities must each have a charge of plus or minus one electronic charge depending on whether the impurity is N or P-type. There is an electric field associated with these charges, since there must be an impurity gradient for diffusion to occur. The electric field exerts a force on these charged particles which gives them a drift velocity, and the product of this drift velocity and the concentration gives another component of flux.

The electric field can be calculated by assuming that the semiconductor is in a thermal equilibrium. There are several orders of magnitude difference in the diffusion coefficients of holes or electrons and impurity atoms. Therefore, the holes or electrons, depending on the type of semiconductor, tend to diffuse away faster than the impurity atoms. The electric field prevents this from happening, so that the impurity current and the hole or electron current are equal. The impurity current is known to be small, since the impurities move on the order of a micron per hour. Then in order to approximate the electric field, the hole current for a P-type semiconductor is set equal to zero.

$$0 = -q D_p \frac{\partial p}{\partial y} + q \mu_p E p \quad (2-11)$$

From equation (2-11), where D_p and μ_p are the diffusivity and mobility of holes respectively, the electric field is obtained as given by equation (2-12).

$$E = \frac{kT}{q p} \frac{\partial p}{\partial y} \quad (2-12)$$

In equation (2-12), D_p/μ_p has been replaced kT/q from the Einstein relation.

The impurity atoms will have a drift velocity which is given by equation (2-13).

$$v = -\mu E \quad (2-13)$$

where μ is the mobility of impurity atoms, and the negative sign indicates that negatively charged particles move in a direction opposite to the direction of the field.

The flux of particles due to the drift velocity, assuming all impurities are ionized, is the product of the concentration of impurities and the drift velocity.

$$F = -\mu EN \quad (2-14)$$

If the electric field, the oxide growth, and diffusion are accounted for, the total flux of particles is the sum of the flux terms given in equations (2-5), (2-6), and (2-14).

$$F = -D \frac{\partial N}{\partial y} - \alpha \frac{dX_o}{dt} N - \mu EN \quad (2-15)$$

From Fick's second law and equation (2-5), the diffusion equation which accounts for oxide growth and field aided diffusion is

$$\frac{\partial N}{\partial t} = D \frac{\partial^2 N}{\partial y^2} + \alpha \frac{dX_o}{dt} \frac{\partial N}{\partial y} + \frac{\partial}{\partial y} (\mu EN). \quad (2-16)$$

To calculate the hole concentration, p , it is assumed that at the high temperatures used for diffusion all impurities are ionized.

The relationship between the hole and impurity concentrations is defined by the following two equations.

$$p = N + n \quad (2-17a)$$

$$pn = n_i^2 \quad (2-17b)$$

Substitution of the electron concentration, n , from equation (2-17a) into equation (2-17b) gives an expression for the hole concentration in terms of the impurity concentration and the intrinsic concentration, n_i .

$$p = \frac{N}{2} + \left(\frac{N^2}{4} + n_i^2 \right)^{1/2} \quad (2-18)$$

If the number of impurities is much greater than the intrinsic concentration, the number of holes is approximately equal to the impurity concentration. For this condition, the diffusion equation can be rewritten using equations (2-12) and (2-15).

$$\frac{\partial N}{\partial t} = D \frac{\partial^2 N}{\partial y^2} + \alpha \frac{dX_o}{dt} \cdot \frac{\partial N}{\partial y} + D \frac{\partial^2 N}{\partial y^2} \quad (2-19)$$

Equation (2-19) shows that the diffusion coefficient is effectively doubled for high impurity concentrations under the influence of a built in electric field. For low impurity concentrations, the number of holes is approximately equal to the number of intrinsic carriers, and the field aided term in the diffusion equation is small.

The electric field adds a term to the flux used in determining the surface boundary condition, equation (2-9). For a predeposition this term may be significant, because of the high surface concentration,

but the boundary condition for predeposition is not calculated from the flux of particles. For drive-in diffusion the temperature is usually much higher, but the intrinsic concentration is also higher.

The temperature dependence of the intrinsic concentration is given by equation (2-20).⁷

$$n_i = 3.85 \times 10^{16} T^{3/2} \exp \left(- \frac{1.21}{2kT} \right) \quad (2-20)$$

For typical drive-in temperatures, n_i is between 10^{19} and 10^{20} , and the surface concentration will be lower than the intrinsic concentration. Since the hole concentration, equation (2-18), is almost constant; the field, given by equation (2-12), is insignificant.

Lehovec and Slobodsky⁸ have investigated field aided diffusion by lumping the diffusion and field terms into a single term with an effective diffusion coefficient, D^* .

$$D^* = D(1+f) \quad (2-21)$$

The function f accounts for the difference in the hole concentration and the impurity concentration. Using this relation to account for the field, they have shown a region of high impurity concentration in which the diffusion coefficient was doubled, and region in which the field was not significant.

Equation (2-10) has been used by Grove⁹ to model diffusion with a growing oxide for wafers with a constant initial doping, and Kato and Nishi¹⁰ have used this equation to approximate the solution for the impurity profile for the more general case.

3. COMPUTATIONAL METHODS

The practical diffusion models require the application of numerical methods to integrate the diffusion equation. This section describes some finite difference methods useful for obtaining solutions. The simplest finite difference method is called the explicit method which is discussed in Appendix I. The method consists of the repeated use of equation (3-1).

$$N_j^{i+1} = RN_{j-1}^i + N_j^i \left\{ 1 - GA + R \left[\frac{P_{j-1}^i - P_j^i}{P_j^i} - 2 \right] + N_{j+1}^i \cdot [GA + R + R \frac{P_{j+1}^i - P_j^i}{P_{j+1}^i} - 1] \right\} \quad (3-1)$$

In equation (3-1) all variables are the same as defined in Appendix I.

The difference approximation becomes more accurate as the increments, Δt and Δy , approach zero; but there are further restrictions for a solution to be convergent. For equation (1-3), the value of R is restricted as is indicated in equation (3-2).

$$R = \frac{\Delta T}{\Delta Y^2} \quad 0 < R < 1/2 \quad (3-2)$$

Assuming a similar relation holds for the more general diffusion equation, equation (3-1) can be used for predicting impurity profiles. Starting with the initial condition, the impurity profile is predicted at the next time instant using the present profile. For each time

step, the values of impurity concentration are calculated at the discrete intervals $j\Delta y$ for all values of j between, but not including, zero and J . These two points must be reserved for the boundary conditions. This will require $J-2$ calculations for each time step. If the total diffusion time is divided into I increments, the $J-2$ calculation must be made $I-1$ times to obtain the final impurity profile.

In calculating the impurity profile by the explicit method, each predicted value of concentration depends only on three previous values as is shown in equation (3-1). The value of R is restricted to certain limits for stable solutions. The implicit method, described in Appendix II, overcomes both of these difficulties; but the ease of computation is lost. A matrix of difference equations must be solved simultaneously, but for this method each predicted value of concentration depends on all of the previous values and on the predicted values. The implicit method should be more accurate than the explicit method because of this increased dependence.

The solution to the diffusion equation is calculated in a way that is similar to the explicit method, except that the entire impurity profile is calculated by solving the matrix equation. A simplified flow diagram that shows the order in which the calculations proceed for a computer solution to the diffusion equation is shown in Figure (3-1). A complete listing of the program used for predicting solutions to the equation by the implicit method is given in Appendix III.

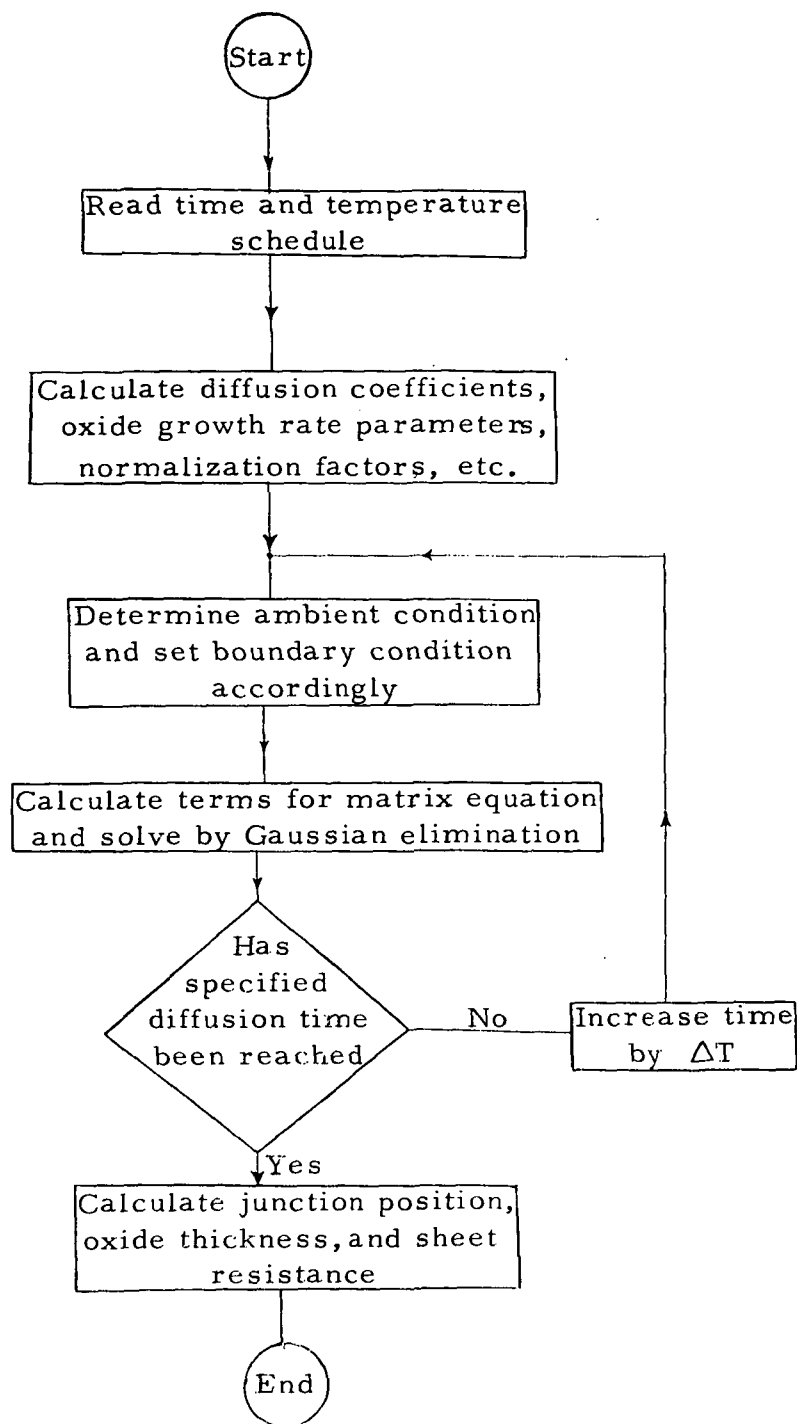


Figure (3-1). A simplified flow diagram for the computer solution of the diffusion equation

The boundary condition at the surface is met by imposing the restriction given by equation (2-9) to calculate the surface concentration. Writing equation (2-9) in finite difference form and solving for the surface concentration gives the equation used to meet the surface boundary condition.

$$N(0, T) = \frac{N(\Delta Y, T)}{\left[1 + \Delta Y \cdot (K - \alpha) \frac{dX_o}{dt} / D \right]} \quad (3-3)$$

The oxide growth rate is calculated from equation (2-1) according to the ambient condition. The ambient condition can be changed during a diffusion and the boundary condition will still be met.

The second boundary condition is that the impurity concentration goes to zero as y approaches infinity. For a numerical solution, some convenient point must be chosen where the impurity concentration is known. If a point is chosen far enough away from the surface, the concentration can be specified to be zero. Since the impurity profile between the surface and the junction is usually the only part that is of interest, the solution will not be significantly affected in this region if the specified point is slightly in error.

For the computer program given in Appendix III, the junction depth is predicted from equation (1-10), and the impurity concentration is set to equal zero at three times the junction depth. This allows the program to handle diffusions for shallow or for very deep

junctions; although, solutions for shallow junctions are more accurate because the increments will be smaller.

Although the predeposition can be numerically simulated to get the initial condition before drive-in, it was found that the impurity profile after the drive-in was not affected significantly by the deviation from a complementary error function, equation (1-5b), during the predeposition. The effect of field aided diffusion is taken into account empirically for the predeposition by adjusting the diffusion coefficient and assuming that the impurity concentration still follows the complementary error function profile. The profile is calculated by taking the integral indicated in equation (1-5a), which is integrated numerically by the Gauss-Laguerre quadrature method.

For the case where a predeposition is not followed by a drive-in, such as the emitter diffusion for a double diffused transistor, the effect of the electric field cannot be accounted for empirically. This type of diffusion can be handled numerically by a slight alteration of the program given in Appendix III.

The sheet resistance is determined by numerical integration of equation (3-4).

$$\frac{1}{R_s} = \int_0^{x_j} G \, dY \quad (3-4).$$

In this equation G is the conductivity which is given as a function of impurity concentration by Irvin.¹¹

4. RESULTS

Both the explicit and implicit methods have been used to solve the diffusion equation. The explicit program has been run on the MSU UNIVAC 1106 and the MSFC Xerox Sigma V. Checks on computational accuracy have been made by comparing with the $\text{erfc}(x)$ and gaussian tables and by comparing with previous work on oxidation done by other methods. Some comparisons with experimental data have also been made. These results are reported in this section.

Solutions by the explicit method were found to be accurate enough for many diffusion problems. It is well suited for the generation of sheet resistance and junction depth data for diffusions in which the ambient condition during a drive-in is constant. The implicit method also works well for drive-ins with one or two ambient changes if the times in each ambient are about equal. If the time in one ambient condition is much greater than another, then the shorter time will be divided into a smaller number of time increments, and the effect of the short ambient change may not show up properly in the solution.

Changing the ambient during a diffusion creates another problem in the stability of the solution. As previously stated, the value of R , $\Delta T / \Delta Y^2$, must be chosen between zero and one half in order to obtain a stable solution to equation (1-3) by the explicit method. If the numerical solution is to be general, then equation (2-16), which accounts for the oxide growth and the electric field, must be

solved. For this equation the range in which R must be chosen for a stable solution may not be the same. For a predeposition, the electric field is significant, but there is no oxide so that an equation different from equation (2-16) is solved. In the case of a drive-in that starts out in an oxidizing ambient, the concentration near the surface drops rapidly. The electric field is negligible, in this case, after the impurity concentration drops below the intrinsic concentration and still another equation is solved.

A single value for R which gives the smallest error for each of these conditions cannot be found for the explicit method. The implicit method should give better results in general because the dependence of solutions on the value chosen for R is greatly reduced. Fewer calculations are required to show the effect of an ambient change, but more computation is required for each prediction of the impurity profile. If one hundred increments in the Y -coordinate are used and R is one fourth, the explicit method requires about three seconds of execution time on the UNIVAC 1106. Under the same conditions, the implicit method requires about thirty seconds of execution time; but by choosing R to be unity, better results are obtained and the execution time is comparable to that of the explicit method.

The solutions given by Grove were simulated numerically for an oxide growing on a wafer with a constant initial background doping

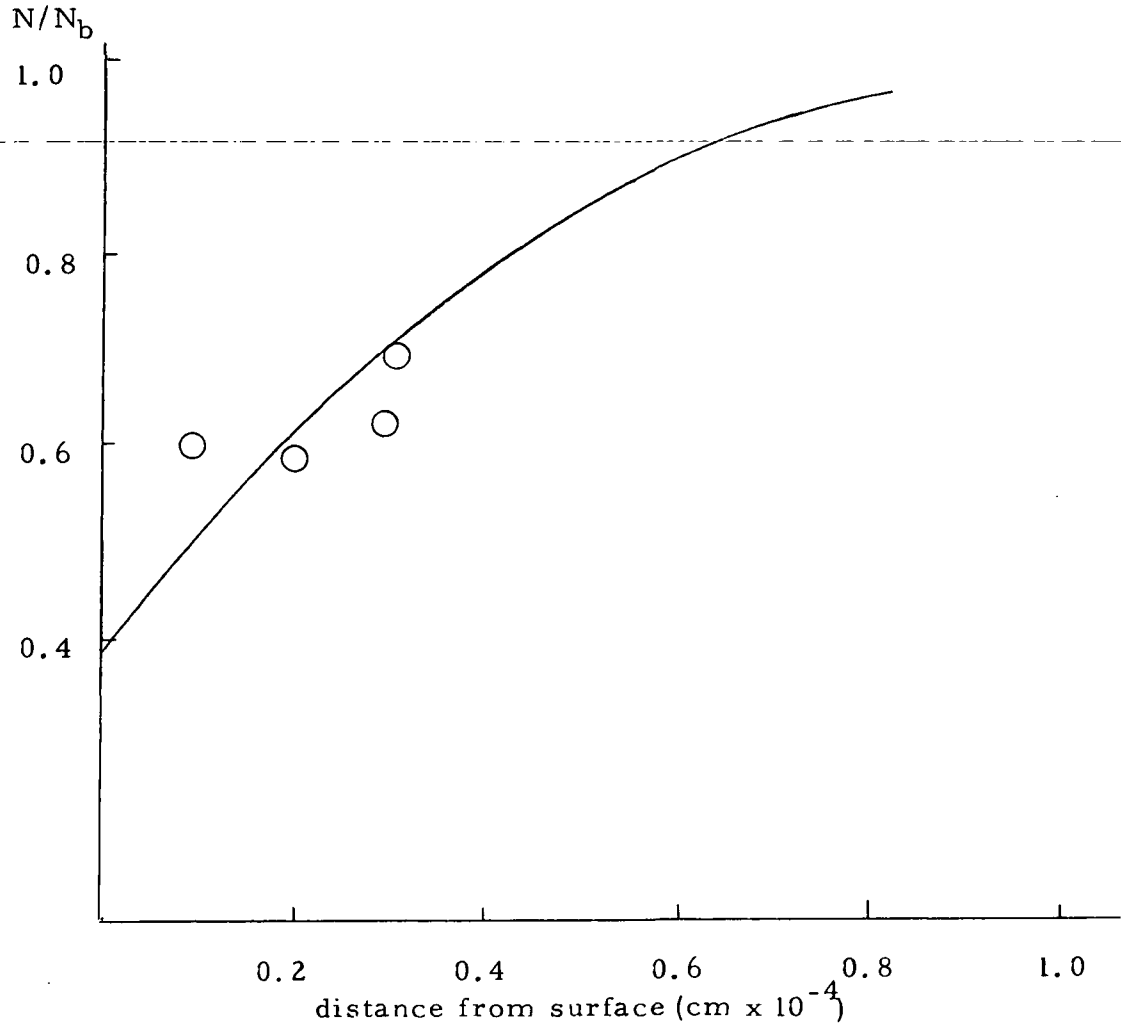


Figure (4-1). Comparison of Predicted Results with the Results of Grove.

level. Since reported values of diffusion parameters vary widely, the diffusion coefficient and segregation coefficient given by Grove was used. The result of this diffusion is given in Figure (4-1).

The circles represent the extremities of experimentally measured concentration.

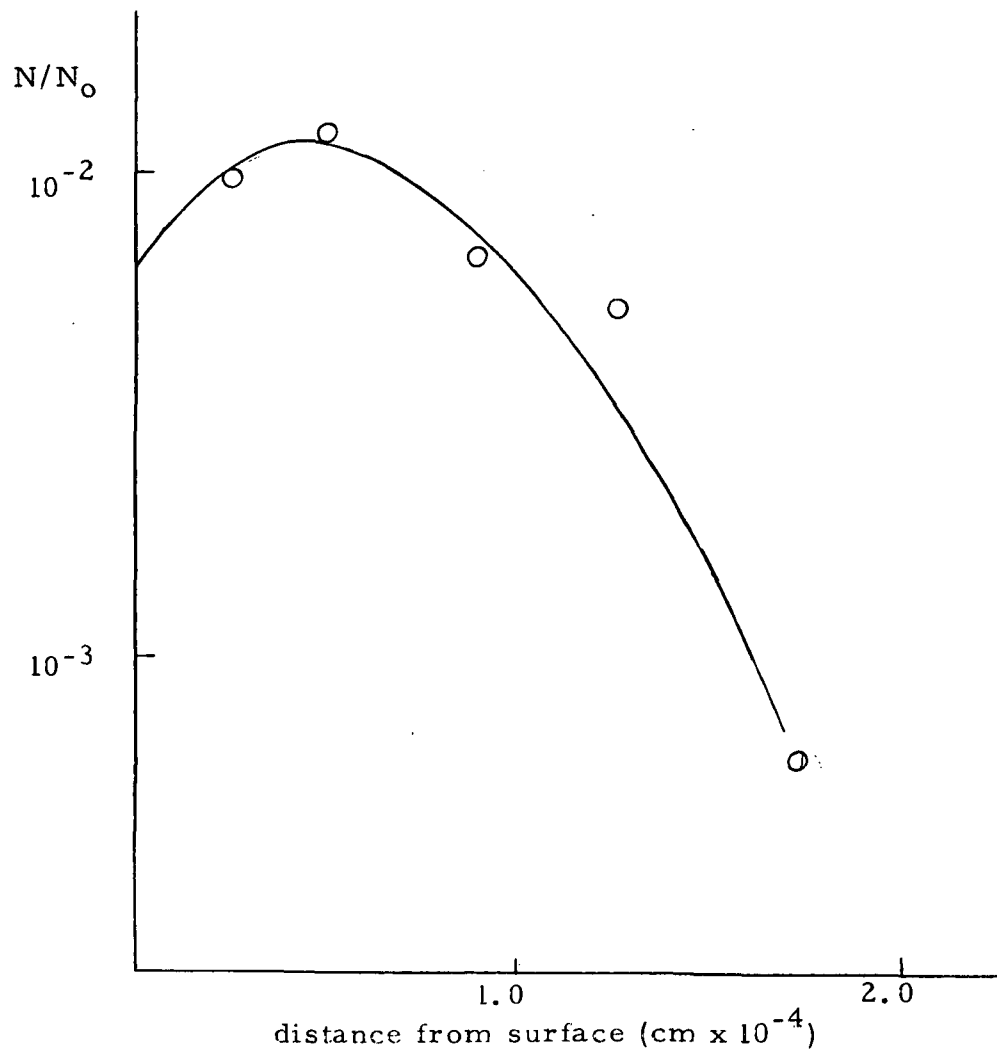


Figure (4-2). Comparison of Predicted Results with the Results of Kato and Nishi

The diffusion data given by Kato and Nishi was also simulated. Figure (4-2) is a comparison of the computer solution and the experimental measurements. The impurity profile given is for a short predeposition followed by a fifty minute drive-in in an oxygen ambient. The diffusion coefficient and segregation coefficient used were the values reported by Kato and Nishi.

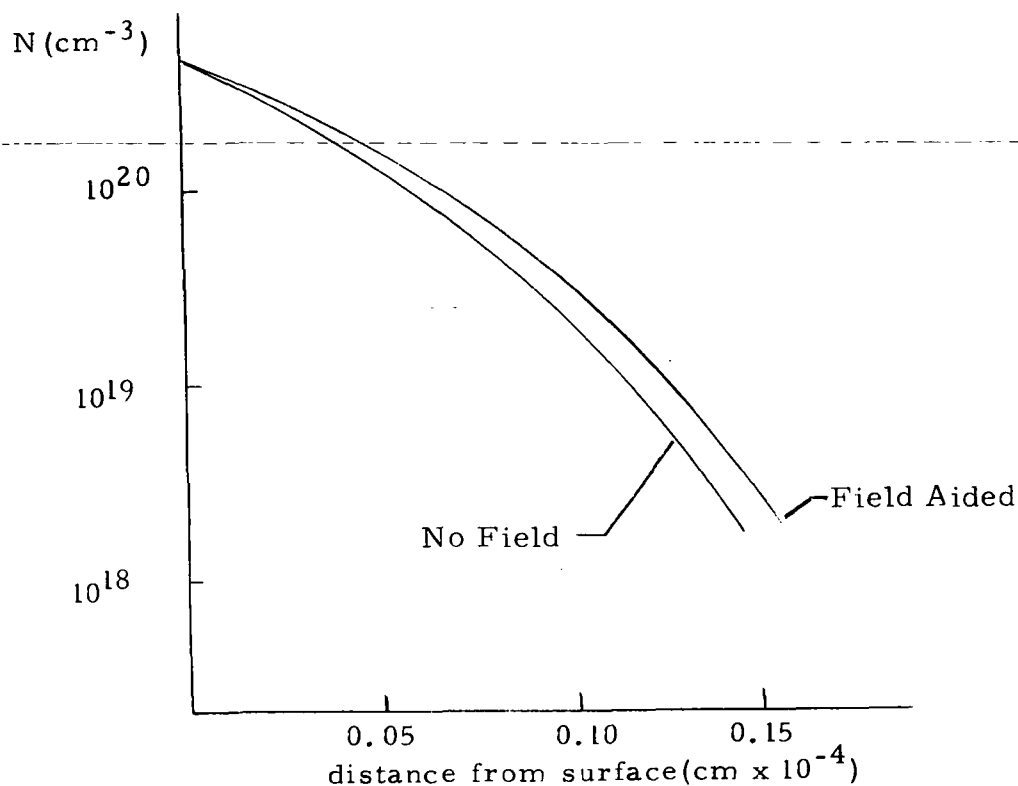


Figure (4-3). The Effect of the Electric Field on a Predeposition.

Figure (4-3) shows a calculated impurity profile with the electric field considered and one in which the field term has been removed from the diffusion equation. These profiles are for a predeposition with boron at 980 degree centigrade for one hour. The most significant difference in these two profiles is that the profile calculated with the field-aided term included shows more impurities in the semiconductor. The effect of these added impurities as a function of the predeposition temperature is shown in figure (4-4). The per cent change in sheet resistance and junction depth were obtained by comparing the results of computations of impurity

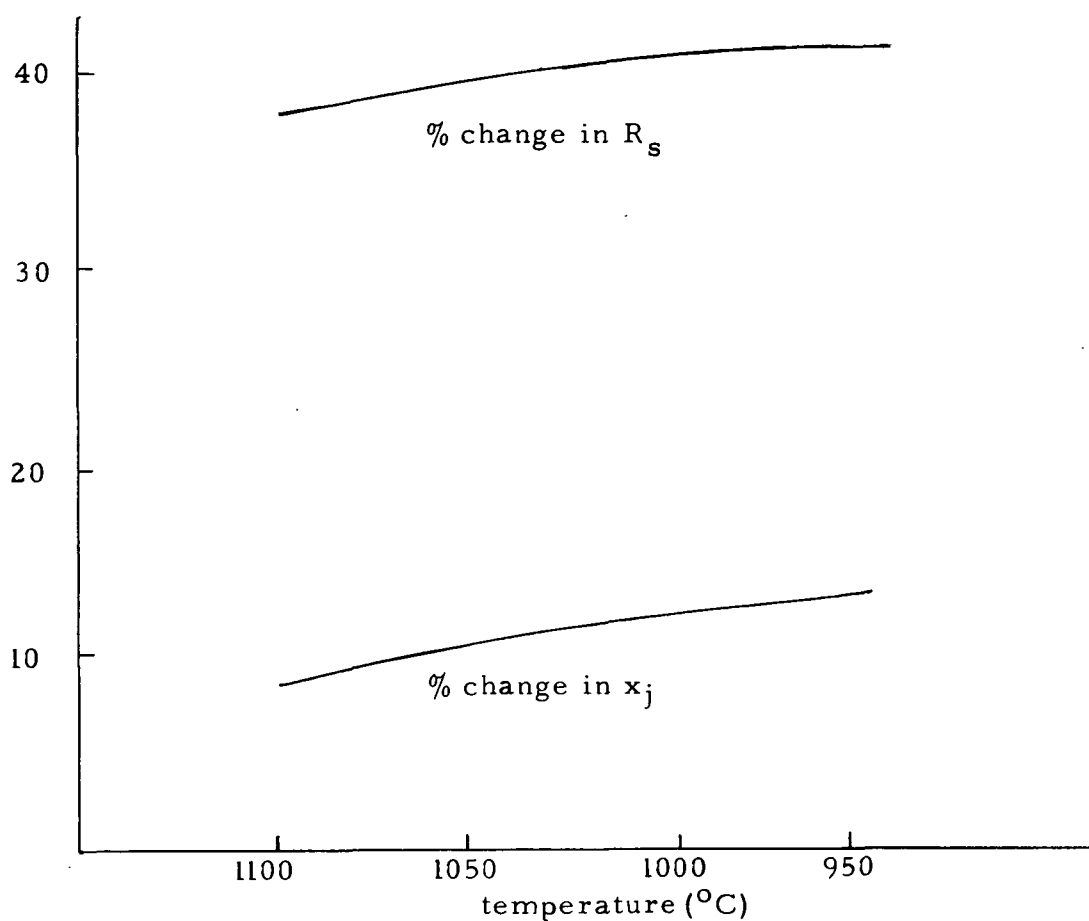


Figure (4-4). The Effect of the Electric Field as a Function of Temperature.

profiles with field aided diffusion and with the field equal to zero. For these calculations the surface concentration was assumed to be constant at 4.0×10^{20} .

In some cases the ambient is changed several times during a diffusion in order to shape the impurity profile to give some desired electrical characteristic. Table (4-1) shows four diffusion schedules with several changes of ambient and a comparison of calculated and experimental values of sheet resistance and junction depth.

AMBIENT
CONDITION

	TIME (MINUTES)			
	(a)	(b)	(c)	(d)
N ₂	14	14	8	8
O ₂	15	15	10	10
H ₂ O	10	10	10	10
O ₂	5	5	5	5
N ₂	10	10	10	10
O ₂	60	0	0	60
N ₂	10	0	0	60
R _s (MEASURED)	160	140	150	200
R _s (CALCULATED)	188	149	172	206
X _j (MEASURED)	2.0	1.3	1.2	2.0
X _j (CALCULATED)	2.08	1.44	1.2	1.98

Table (4-1). Some Predicted and Experimental Results for Several Ambient Changes.

Some results which show the effect that the oxide growth has on impurity profiles as time progresses are shown in Figures (4-5) and (4-6). Figure (4-5) shows that for phosphorus the oxide rejects the impurities and pushes them inward keeping the concentration near the surface relatively high. For the boron profile, Figure (4-6), the concentration near the surface is depleted. A comparison of the two figures shows that the boron profile contains fewer impurities than the phosphorus profile.

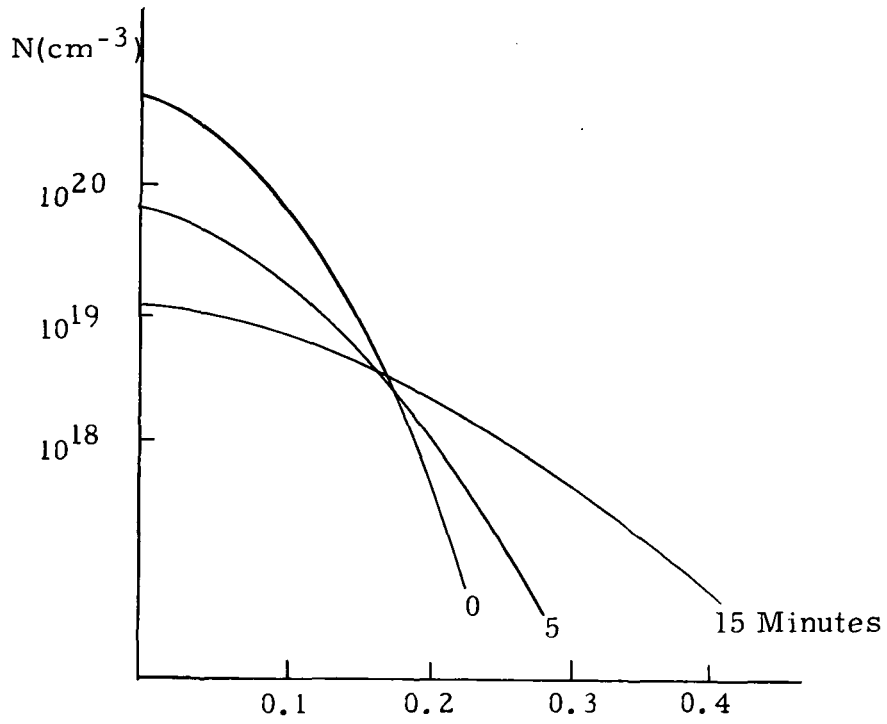


Figure (4-5). Profile Evolution for Phosphorus in an Oxidizing Ambient

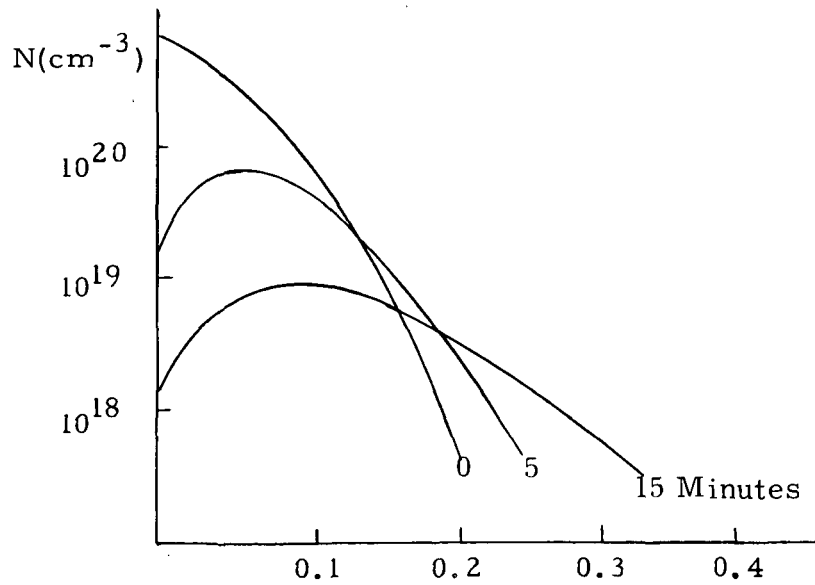


Figure (4-6). Profile Evolution for Boron in an Oxidizing Ambient

5. PREDEPOSITION DIFFUSIONS

There are several methods used for accomplishing the pre-deposition diffusion: (1) a gaseous impurity source such as diborane or phosphine is mixed with carrier gases of nitrogen, oxygen, and argon; (2) a liquid source such as POCl_3 is used with a carrier gas mixture which bubbles through the liquid; (3) a solid source such as boron nitride wafers or P_2O_5 is used with a carrier gas; (4) a doped oxide source is deposited on the wafer surface either by pyrolytic techniques or by "spin-on" methods using a liquid emulsion which is dried and baked.

The first three methods require that the surface concentration be maintained at the solid solubility limit in order to obtain control of the impurity profiles. High surface concentrations result in lattice strains which are not always annealed out by subsequent drive-in diffusions. These lattice strains may produce deleterious effects in terms of device performance. Consequently, there has recently been a good deal of interest in method (4) which can produce predeposition profiles with acceptable control and lower surface concentrations. The other methods are also widely used and method (1) was studied in this work.

The diborane predeposition procedure is usually carried out in a furnace at about $1,000^\circ\text{C}$. (980°C . in the furnace at MSFC.) The carrier gases are N_2 , at 4,000cc/min flow rate, O_2 , at 120cc/min, and argon at 22cc/min with 1 percent diborane in the argon. The

diborane argon mixture is supplied for times ranging from about 15 minutes to 60 minutes. A layer of boron glass (B_2O_3) is formed with a thickness up to about 1,200 Angstroms. This layer is quickly dissolved in a 10:1 HF etch. There is an inter-layer which is a solid mixture of boron-silicon-oxygen which is resistant to the HF etch. The layer ranges from about 100 to more than 200 Angstroms according to ellipsometer measurements (which may not be reliable.)

Exactly how much of this recalcitrant layer that remains after the 10:1 HF etch is dependent upon the time used for the predeposition. The data obtained at this time indicates that for a 15 minute predeposition, the layer is almost completely etched away in HF. The surface sheds water readily, and a subsequent short drive-in diffusion in N_2 does not produce a dramatic drop in the sheet resistance. For a 30 or 60 minute predeposition, the layer which remains after an HF etch is about 200 Angstroms thick, water clings to the surface, and a short drive-in in N_2 (5-10 minutes) produces a drop in the sheet resistance by a factor of four. An etch cycle in hot ($105^\circ C$) nitric followed by a 10:1 HF etch is effective in removing the layer. Three cycles seemed to be sufficient. A short oxidation (5 minutes) at $1150^\circ C$ followed by a 10:1 HF etch is also effective in removing the layer.

Wafers which were predeposited for 30 and 60 minutes were divided into two groups. Half of the wafers were etched (HNO_3+HF) and half were not. These wafers were then subjected to drive-in

diffusions in N_2 at $1150^\circ C$. for a total time of 50 minutes. The wafers were removed at intervals and the sheet resistance checked. Of course, there is an ambiguity concerning the effective time because of the heating and cooling times; however, the results are shown in Figure 5.1. Apparently, the boron-rich interlayer serves as an effective unlimited source for a period of 50 minutes. Since the chemical composition of the interlayer is unknown, any calculation of the total number of impurities based on the layer thickness must be considered to be purely speculative. An estimate based on the assumption that the layer is roughly a 50 percent mixture of B_2O_3 and SiO_2 gives $10^{16} cm^{-2}$ for the effective Q of the source. This is sufficient to maintain a saturated surface concentration for roughly an hour at $1150^\circ C$.

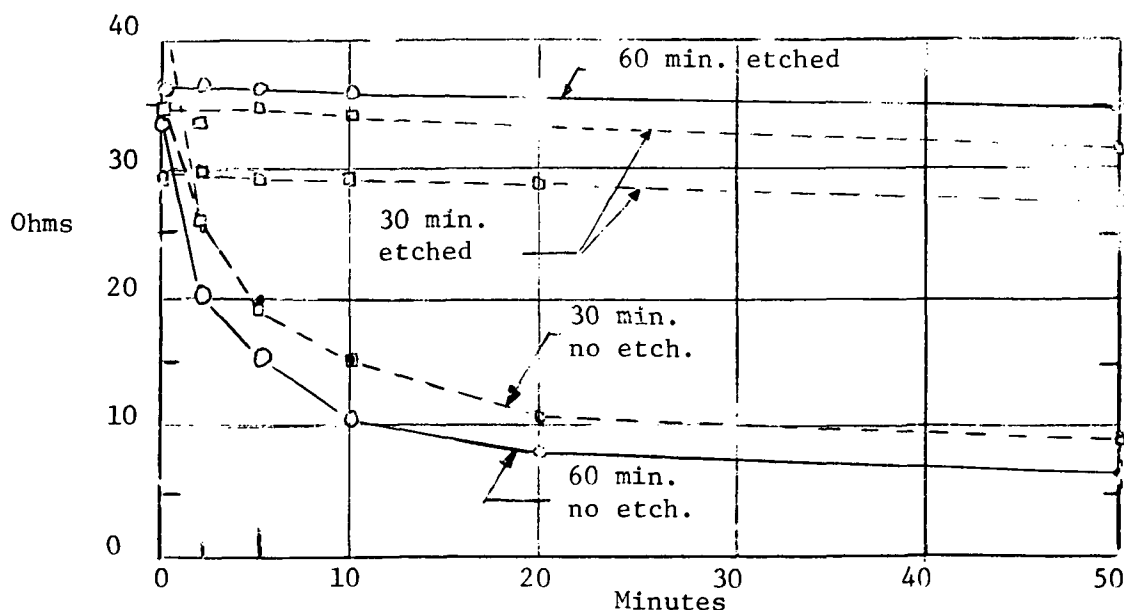


Figure 5.1 Sheet Resistance vs. Time for Drive-in Diffusion in Nitrogen at $1150^\circ C$ with Boron-Rich Surface Layer.

If the wafers with the boron-rich interlayer are placed into an oxidizing ambient, either dry oxygen or steam, the results are quite different. The sheet resistance at first holds steady with the drive-in time and then begins to increase. The increase will continue until such a time that the impurity gradient at the junction is too low to maintain a space charge layer. Then the junction becomes "leaky" and the resistance measured is no longer related directly to the resistance of the diffused P-layer above the junction. Apparently, the oxide begins to grow between the boron-rich layer and the silicon, and, no doubt, some transformation takes place within the layer. Consequently, the layer is masked from the silicon, and probably dilated, so that it no longer supplies impurities at a rate which maintains a saturated surface concentration.

The best model which one can construct at this time on the basis of the available data is as follows. An effective surface source with strength Q_{s1} (cm^{-2}) is assumed for all predeposition times between 30 and 60 minutes. The value chosen for Q_{s1} is approximately $3.5 \times 10^{16} \text{ cm}^{-2}$. For 15 minutes or shorter predep times, $Q_{s1} = 0$. In order to incorporate this predep model into the overall two-step diffusion model, the following scheme is employed: (1) For a drive-in in a N_2 ambient, the flux of impurities at the surface is calculated and integrated with respect to time. The surface concentration is assumed to be at the solid solubility limit until the integrated flux is equal to Q_{s1} . Then the flux is set to zero. If Q_{s1}

is incorrect, then the model eventually becomes invalid. However, in most practical cases only a short drive-in in N_2 is required, so that this is not a severe limitation. (2) For a drive-in in an oxidizing ambient, the surface flux is assumed to be zero until an oxide 800 Angstroms thick is grown. Then the flux is assumed to follow the law dependent upon the oxide growth rate, the segregation coefficient, etc. The model is to some extent arbitrary, and other models may give equivalent results. A more rigorous approach would deal with the chemical conversion of the interlayer plus the oxide growth and diffusion through the oxide. This is obviously a very involved problem requiring micro-chemical analysis of thin layers for boron, silicon, and oxygen content. Until such empirical data are available, the present model is no more nor less speculative than any other.

The curves given in Appendix V for diborane predepositions without removal of the boron-rich layer were obtained using the model described in the preceding paragraph. The curves are calculated using the "explicit" integration program which is given in Appendix IV. The program as given has a set of instructions to generate the input data. These instructions may be easily replaced with read instructions or other instructions to input the data. The program uses the following data: (1) RS_1 , the sheet resistance after the predeposition, (2) TE_1 , TI_1 , the predep temperature and time (degree C., and minutes,) (3) TE_2 , the drive-in temperature (deg. C), (4) T_1 , T_2 , T_3 ,

the drive-in are obtained by assuming that the field-aided diffusion during the predep results in an effective diffusion constant of $2D$. Then the surface concentration is adjusted to give the correct sheet resistance for the predep, RS_1 . This is done by a subprogram called $FINDNO(RS_1, LA, NO)$. Practically, this usually results in a junction depth after the predep which is too deep and gives a bias to the junction depths for drive-in. Sheet resistance values seem to agree fairly well. The junction depth error is roughly .2 microns for a 60 minute predep.

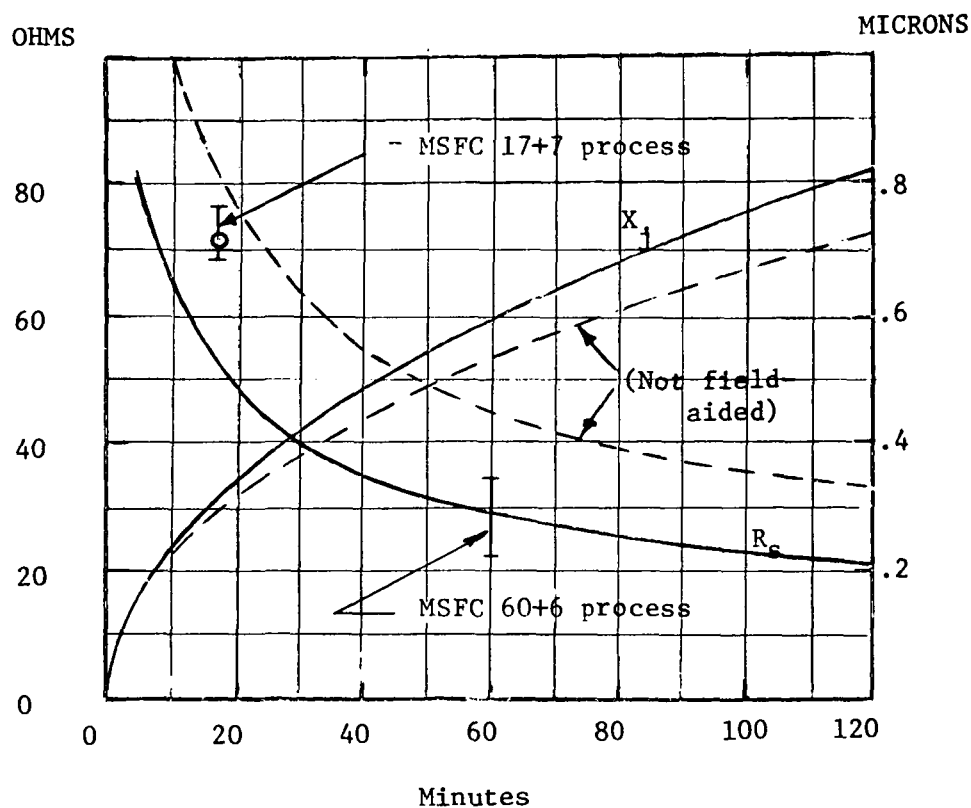


Figure 5.2 Sheet Resistance and Junction Depth vs. Time for B_2H_6 , Diborane, Predeposition Diffusion.

(Circled point calculated by including time in O_2)

The sheet resistance after the predep can be calculated fairly accurately by taking into account the aiding electric field. Curves are shown in Figure (5.2) for sheet resistance versus predep time at 980°C. It is questionable whether or not it is practical to calculate the predep profile using the program including the field aided effect each time the drive-in profile is calculated. There are several difficulties which must be resolved, one being the problem of reconciling the two choices of "regions for the solution." If one chooses a reasonable region for solving the drive-in problem, this region is inevitably too large for an accurate numerical integration for the predep profile. On the other hand, choice of two regions, one for predep and one for the drive-in, requires a coordinate transformation type of operation to translate data calculated using a finer grid to a description with a coarser grid. However, one accomplishes this, extra computing time and added program complexity are required. At the moment it is not certain that the increase in accuracy warrants this approach, but it is being considered. It seems now that the most practical approach is to use the sheet resistance data as input data to solve the drive-in problem.

The "explicit" program can also be used to simulate predepositions using boron-nitride wafers for diffusion sources. In this case, the predep sheet resistance is calculated from formulas based on Goldsmith's (et. al.) data.¹³ For this option, the control index ICON is set equal to zero.

6. CONCLUSIONS AND RECOMMENDATIONS

The model and program described in this report is useful for calculating junction depths and sheet resistances for practical two-step diffusion processes. In cases where the model has been compared with empirical data, the results for junction depths have agreed to within less than 10 percent, better than the uncertainty of measurement for some individual measurements. Sheet resistance data agrees well in some cases. Experimental data shows that the sheet resistance after a diborane predep is sometimes erratic. Variations of as much as 8ohms from the average of 27 ohms for a 60 minute diborane predep have been observed. The program cannot, of course, cope with this problem. More controllability of the process is needed and this requires more understanding of the physics and chemistry of the process. When the experimental values for the predep sheet resistance are used to predict the value after drive-in, the predicted value agrees within 10 percent of the measured value.

There are some practical effects known to be missing from the model. The non-linearity introduced with very heavy phosphorous concentrations and resulting in the "emitter-dip" phenomena are not modeled in the program. This is not a severe limitation for diffusions used for MOST devices. There is also a tendency to get away from this type of diffusion because of the deleterious effects produced as well as the unpredictable nature of the process. The complexity of the conversion of the impurity-rich interlayer upon

subsequent oxidation has not been modeled. More experimental data will be required before a more accurate model can be constructed.

One feature of the model which is deficient and will be subsequently remedied is in the method of calculating the sheet resistance. The sheet resistance is obtained by integrating the conductivity from the surface to the junction. Some of the data in Appendix V are obtained using the resistivity of the diffused concentration rather than the net concentration. In most cases, this does not matter, but for a light doping it will. The other problem is that the junction becomes leaky when the impurity concentration is light and the gradient at the junction is low. A calculation for the impurity gradient at the junction will be inserted to indicate when the calculations are unreliable. Practically such a diffusion is useless, but one would wish to know when such results will be obtained.

Additional studies should be made to apply these programs to diffusions from doped oxides and from the boron-nitride type source. Curves can be obtained for the boron-nitride predepositions and the program can be used to study the P-well diffusions used in CMOS work. This problem is very difficult because the P-region must be lightly doped and the junction must be deep. Consequently, it is very difficult to produce a junction which is not leaky or "lost" altogether because the diffused region becomes N-type.

Further studies are needed to improve the model for the impurity-rich interlayer. In this case, data are needed to learn

what is actually happening physically. Chemical analysis of the layer before and after oxidation is needed. The program should be modified so that the predep profiles calculated using the field-aided model are readily incorporated into the computations for the drive-in diffusion. Subsequent work will integrate the features of the explicit and implicit programs and utilize the field-aided predep model if the accuracy improvement is felt to warrant the complication.

At this point the programs can be used to simulate a variety of diffusions and for experimentation. Further attention will be given to simplifying the procedures for using the programs. This will probably result in several programs, each incorporating the basic integrated program mentioned above but differing in the input data and output data instructions.

REFERENCES

1. A. M. Smith, Fundamentals of Silicon Integrated Device Technology, Vol. 1., ed. Robert M. Burger and R. P. Donovan, Englewood Cliffs: Prentice-Hall, 1967, p. 187.
2. Ibid., p. 189.
3. Ibid., p. 195.
4. A. S. Grove, Physics and Technology of Semiconductor Devices, John Wiley and Sons, Inc., New York, 1967, pp. 28-29.
5. Ibid., p. 70.
6. A. S. Grove and others, "Redistribution of Acceptor and Donor Impurities During Thermal Oxidation of Silicon," Journal of Applied Physics, September, 1964, Vol. 35, pp. 2695-2701.
7. W. R. Runyan, Silicon Semiconductor Technology, McGraw-Hill Book Co., New York, 1965, p. 164.
8. Kurt Lehovec and Alexis Slobodskoy, "Diffusion of Charged Particles Under Consideration of the Built-in Field," Solid-State Electronics, 1961, Vol. 3, pp. 45-50.
9. A. S. Grove and others, pp. 2695-2701.
10. Taketoshi Kato and Yashio Nishi, "Redistribution of Diffused Boron in Silicon by Thermal Oxidation," Japanese Journal of Applied Physics, Vol. 3, pp. 377-383, 1964.
11. John C. Irvin, "Resistivity of Bulk Silicon and of Diffused Layers in Silicon," The Bell System Technical Journal, March, 1962, Vol. XLI, pp. 387-410.
12. M. L. Barry and P. Olofsen, "Advances in Doped Oxides as Diffusion Sources," Solid State Technology, October, 1968, Vol. 11, No. 10, pp. 39-42.
13. N. Goldsmith, J. Olmstead, and J. Scott, Jr., "Boron Nitride as A Diffusion Source for Silicon," RCA Review, pp. 344-350, June, 1967.

BIBLIOGRAPHY

1. M. L. Barry and P. Olofsen, "Advances in Doped Oxides as Diffusion Sources," *Solid State Technology*, Vol. 11, No. 10, pp. 39-42, October, 1968.
2. M. L. Barry and P. Olofsen, "Doped Oxides as Diffusion Sources," *J. Electrochem. Soc.: Solid State Science*, Vol. 116, No. 6, pp. 854- 860, June, 1969.
3. R. M. Burger and R. P. Donovan (Editors,), Fundamentals of Silicon Integrated Device Technology, Vol. I, Section II, "Diffusion" by A. M. Smith, Prentice-Hall, Englewood Cliffs, N. J. , 1967.
4. K. M. Busen, W. A. FitzGibbons, W. K. Tsang, "Ellipsometric Investigation of Boron-Rich Layers on Silicon," *J. Electrochem. Soc.: Solid State Science*, Vol. 115, No. 3, pp. 291-294, March, 1968.
5. T. L. Chu and G. A. Gruber, "Doped Silicon Films," *Electro Chemical Technology*, Vol. 5, No. 1-2, p. 43-46, Jan-Feb, 1967.
6. C. S. Fuller and J. A. Ditzenberger, "Diffusion of Donor and Acceptor Elements in Silicon," Vol. 27, No. 5, pp. 544-553, May, 1956.
7. N. Goldsmith, J. Olmstead, and J. Scott, Jr., "Boron Nitride as A Diffusion Source for Silicon," *RCA Review*, pp. 344-350, June, 1967.
8. A. S. Grove, Physics and Technology of Semiconductor Devices, Chapter. 2, (Thermal Oxidation), Chap. 3 (Solid State Diffusion,) John Wiley and Sons, New York, 1967.
9. A. S. Grove, O. Leistiko, and C. T. Sah, "Redistribution of Acceptor and Donor Impurities During Thermal Oxidation of Silicon," *J. Applied Phys.*, Vol, 35, No. 9, pp. 2695-2701, September, 1964.
10. M. S. R. Heynes, "Boron Diffusion into Silicon Using Diborane," *Electrochemical Technology*, Vol. 5, No. 1-2, pp. 25-33, January-February, 1967.

11. Shiro Horiuchi and Jiro Yamaguchi, "Diffusion of Boron in Silicon Through Oxide Layer," *Japanese Jour. of Applied Phys.*, Vol. 1, No. 6, pp. 314-323, December, 1962.
12. John C. Irwin, "Resistivity of Bulk Silicon and of Diffused Layers in Silicon," *Bell Systems Tech. Jour.*, Vol. XLI, No. 2, pp. 387-410, March, 1962.
13. T. Kato and Y. Nishi, "Redistribution of Diffused Boron in Silicon by Thermal Oxidation," *Japanese Journal of Applied Phys.*, Vol. 3, pp. 377-383.
14. D. P. Kennedy and P. C. Murley, "Impurity Atom Distribution from a Two-step Diffusion Process," *Proc. of IEEE*, Vol. 52, No. 5, pp. 620-621, May, 1964.
15. James S. Kesperis, "The Effect of Gas Concentration in the Diffusion of Silicon from a Phosphine Source," *J. Electrochem. Soc.: Solid State Science*, Vol. 117, No. 4, pp. 554-557, April, 1970.
16. A. D. Kurtz and R. Yee, "Diffusion of Boron into Silicon," *J. Applied Phys.*, Vol. 31, No. 2, pp. 303-305, Feb., 1960.
17. K. Lehovec and A. Slobodsky, "Diffusion of Charged Particles Under Consideration of a Built-in Field," *Solid State Electronics*, Vol. 3, 1961.
18. W. R. Runyan, Silicon Semiconductor Technology, McGraw-Hill, New York, 1965.
19. Guenter H. Schwuttke, Semiconductor Junction Properties as Influenced by Crystallographic Imperfections, Report No. AFCRL-67-0564, prepared for Air Force Cambridge Research Lab by IBM.
20. W. M. Whittlemore and G. M. Oleszek, The Effects of Process Variables on the Open-Tube Diffusion of Boron Into Silicon From Boron Tribromide, IBM Report, TR 01.1111, December, 1968.

APPENDIX I

NORMALIZATION AND EXPLICIT DIFFERENCE APPROXIMATION

The diffusion equation is normalized so that it can be written in terms of dimensionless time and space coordinates. The normalization factors are given in the following two equations;

$$Y = \frac{y}{\sqrt{D\tau}} \quad (6-1)$$

$$T = \frac{t}{\tau} \quad (6-2)$$

where τ is the total diffusion time.

Writing an equation with this type of normalization facilitates the choice of increments to be used in a numerical solution.

The equation is normalized by using the chain rule for differentiation. As an example, the time derivative is rewritten as follows;

$$\frac{\partial N}{\partial t} = \frac{1}{\tau} \cdot \frac{\partial N}{\partial T} \quad (6-3)$$

The normalized diffusion equation is given in the following equation.

$$\frac{\partial N}{\partial t} = \frac{\partial^2 N}{\partial Y^2} + \frac{\tau}{D} \cdot \alpha \frac{dX}{dt} \cdot \frac{\partial N}{\partial Y} + \frac{\partial}{\partial Y} \left(\frac{\partial p}{\partial Y} \frac{N}{p} \right) \quad (6-4)$$

The time and space derivatives are approximated by finite differences.

$$\frac{\partial N}{\partial T} = \frac{N_j^{i+1} - N_j^i}{\Delta T} \quad (6-5)$$

$$\frac{\partial N}{\partial Y} = \frac{N_{j+1}^i - N_j^i}{\Delta Y} \quad (6-6)$$

The superscripts $i+1$, i , and $i-1$ indicate that N is evaluated at times $T + \Delta T$, T , and $T - \Delta T$ respectively. The j subscripts are analogous for the spatial coordinate.

Substituting the finite differences into the diffusion equation gives the following difference equation.

$$N_j^{i+1} = N_{j-1}^i + R + N_j^i \left[1 - GA + R \left[\frac{p_{j-1} - p_j}{p_j} - 2 \right] \right] + N_{j+1}^i \left[GA + R + R \frac{p_{j+1} - p_j}{p_{j+1}} \right] \quad (6-7)$$

$$R = \frac{\Delta T}{\Delta Y^2}$$

$$GA = \frac{\tau \Delta T}{\sqrt{D\tau} \Delta Y} \propto \frac{dX_o}{dt}$$

In equation (6-7) all unsuperscripted variables are assumed to be evaluated at time T .

With the first and last values of N given from the boundary conditions, the difference equation can be used iteratively to predict the impurity profile at the next time instant if the present profile is known.

APPENDIX II

IMPLICIT DIFFERENCE METHOD

The implicit method is similar to the explicit method except that the spatial derivatives are written in terms of the impurity concentration at the next instant of time.

$$\frac{\partial N}{\partial Y} = \frac{N_{j+1}^{i+1} - N_{j-1}^{i+1}}{2 \Delta Y} \quad (7-1)$$

$$\frac{\partial^2 N}{\partial Y^2} = \frac{N_{j+1}^{i+1} - 2N_j^{i+1} + N_{j-1}^{i+1}}{\Delta Y^2} \quad (7-2)$$

Substituting the finite difference derivatives into the diffusion equation gives the following difference equation.

$$\begin{aligned} N_j^i = & N_{j-1}^{i+1} \left[R - R/4 (p_{j+1}^i - p_{j-1}^i) / p_{j-1} - GA/2 \right] + N_j^{i+1} \left[-1 - 2R \right. \\ & \left. + R (p_{j+1}^i - 2p_j^i + p_{j-1}^i) / p_j \right] + N_{j+1}^{i+1} \left[R + R/4 (p_{j+1}^i - p_{j-1}^i) / p_{j+1} \right. \\ & \left. + GA/2 \right] \end{aligned} \quad (7-3)$$

In equation (7-3) there are three unknowns, i. e., the three values of impurity concentration. If j runs from zero to J , where $J\Delta Y$ is the largest value of Y to be considered, then there are $J-2$ equations in $J-2$ unknowns to be solved simultaneously. These equations can be written in the form of a matrix equation as is shown in equation (7-4).

$$\begin{bmatrix} N_1^i - AN_0^{i+1} \\ N_2^i \\ N_3^i \\ \cdot \\ \cdot \\ \cdot \\ N_{J-2}^i \\ N_{J-1}^i - CN_J^{i+1} \end{bmatrix} = \begin{bmatrix} B & C & & & & & & & \\ & A & B & C & & & & & \\ & & & & A & B & C & & \\ & & & & & & & \cdot & \\ & & & & & & & \cdot & \\ & & & & & & & \cdot & \\ & & & & & & & & A & B & C \\ & & & & & & & & & & A & B \end{bmatrix} \begin{bmatrix} N_1^{i+1} \\ N_2^{i+1} \\ N_3^{i+1} \\ \cdot \\ \cdot \\ \cdot \\ N_{J-2}^{i+1} \\ N_{J-1}^{i+1} \end{bmatrix} \quad (7-4)$$

In this equation A, B, and C are the coefficients of N_{j-1} , N_j , and N_{j+1} respectively; and they vary in both time and space. Since the coefficient matrix is tridiagonal, equation (7-4) can be easily solved by Gaussian elimination for all of the next values of impurity concentration. The first and last elements of the column vector on the left-hand side of equation (7-4) each contain two terms. The boundary conditions determine the second term in both cases; and since the boundary conditions are included in the matrix, the solution to equation (7-4) will depend on these boundary conditions.

APPENDIX III

IMPLICIT PROGRAM LISTING

```

C   PROGRAM FOR CALCULATING IMPURITY PROFILE, JUNCTION DEPTH,
C   AND SHEET RESISTANCE FOR TWO STEP DIFFUSION IN SILICON
      DIMENSION N(200), A(200), B(200), E(200), DA(200), CON(200)
      REAL NB, LA, NB, N
      REAL*8 N3, ANM1, ANP1, A0
      NI(T)=EXP(21.25)/((300.0)**(1.5))*1.5E10*EXP(-(6420.
*-2.08*T)/T)*T**(1.5)
      RA(N3, N4)=N3/2.+SQRT(N3**2/4.+N4**2)
C   NB IS THE BACKGROUND DOPING , PER CC
      NB=1.0E15
C   PREDEP TIME(MIN), TEMP(DEG.C.), DRIVE-IN TEMP(DEG.C.),
C   TIME IN N2(MIN), O2(MIN), AND STEAM(MIN)
C   PD IS 1.0 FOR PREDEP.-----0.0(OR BLANK) OTHERWISE
C   TOT IS TOTAL DRIVE-IN TIME IN MINUTES
40  READ(5,10)TI1,TE1,TE2,T1,T2,T3,PD,TOT
10  FORMAT(8F10.3)
      IF(PD.GT.0.)XK=0.0
      WRITE(6,501)TI1,TE1,TE2,T1,T2,T3
301  FORMAT(' ',6E10.2)
      IF(TI1.LE.0.0)STOP
      D1=8.0*EXP(-42.E3/(TE1+273.0))

```

```

TI1=TI1*60.0
TOT=TOT*60.0
T2=T2+T1
T3=T3+T2
T1=T1*60.0
T2=T2*60.0
T3=T3*60.0
C   CALCULATION OF OXIDE GROWTH RATE PARAMETERS
CO=0.171*EXP(-23.1E3/(TE2+273.))
CS=2.37*EXP(-22.7E3/(TE2+273.))
BS=0.652E-9*EXP(-8.2E3/(TE2+273.))
BO=2.14E-9*EXP(-14.4E3/(TE2+273.))
TI2=T3
C   DIFFUSION CONSTANT CM**2/SEC (BORON GIVEN)
D=.4*EXP(-40.5E3/(TE2+273.))
IF(PB.61..91)TI2=D1/D*TI2
IF(TI2.LE.0.0)GO TO 6
LA=2.0*SQRT(D1*TI1)
NO=4.E20
Q=NO*LA*.564
ALPHA=0.45
C   GAUSSIAN ESTIMATION OF JUNCTION DEPTH
XJ=(4.*D*TOT*ALOG(Q/(NB*(5.14*D*TOT)**(.5))))**(.5)
C   CALCULATION OF NORMALIZATION FACTORS
X0=SQRT(D*TOT)
DX=3.*XJ/(100.*X0)
DT=DX**2

```

```

RT=DT*TOT
RX=DX*X0
M=IFIX(1./DT)
-----
M=M*TI2/TOT
J=IFIX(3.*XJ/(X0*DX))
X=0.
IF(PD.LT.1.0)GO TO 300
C   SET INITIAL CONDITION FROM COMPLEMENTARY ERROR FUNCTION
DO 1 I=1,J
N(I)=N0*ERFC(X/(SGRT(D1*T1)*2.0))
X=X+DX*X0
1 CONTINUE
GO TO 40
300 CONTINUE
L=2
R=DT/(DX**2)
DO 3 L=1,M
C   DETERMINATION OF AMBIENT CONDITION
IF(L*RT.LT.T3)COX=CS
IF(L*RT.LT.T2)COX=CO
IF(L*RT.LT.T3)BOX=BS
IF(L*RT.LT.T2)BOX=B0
DX0=BOX/(BOX/COX+2.*XK)
IF(L*RT.LT.T1)DX0=0.
XK=XK+DX0*RT
JO=J-1
N(J)=0.0

```

```

C   SET BOUNDARY CONDITION ACCORDING TO AMBIENT CONDITION
N(1)=N(2)/(RX*(3.3-ALPHA)*DX0/D+1.0)
IF(PD.GT.0.95) N(1)=NO
DO 2 I=2,JO
GA=.45*RT/RX*DX0
ANM1=DBLE(N(I-1))
ANP1=DFLE(N(I+1))
T=TE2
IF(PD.GT.0.) T=TE1
C   CALCULATE INTRINSIC CARRIER CONCENTRATION
AO=NI(T+273.0)
AO=NI(TE2+273.0)
AO=DBLE(AO)
N3=DBLE(N(I))
C   CALCULATE HOLE CONCENTRATION
RAN1=RA(ANM1,AO)+1.0
RAN2=RA(ANP1,AO)+1.0
RAN=RA(N3,AO)+1.0
IF(L.LT.2) RAN=1.0
IF(L.LT.2) RAN1=1.0
IF(L.LT.2) RAN2=1.0
C   CALCULATE TERMS FOR MATRIX EQUATION
A(I)=-R/4.*(RAN2-RAN1)/RAN1-GA/2.0+R
B(I)=-1.0-2.*R+R*(RAN2-2.*RAN+RAN1)/RAN
E(I)=R/4.0*(RAN2-RAN1)/RAN2+GA/2.0+R
DA(I)=-N(I)
2 CONTINUE

```

```

C      CALL SUBROUTINE FOR SOLVING MATRIX EQUATION
      DA(2)=DA(2)-A(2)*N(1)
      DA(J0)=DA(J0)-E(J0)*N(J)
      CALL TRIDAG(2, J0,A,B,E ,DA,N)
3     CONTINUE
      GO TO 40
4     CONTINUE
6     CONTINUE
      DO 5 I=2,J
      C=N(I-1)
C      G(C) FITS IRVINS DATA FOR CONDUCTIVITY
      CON(I-1)=G(C)
      Y=I*RX-2.*RX
      N1=I-1
      WRITE(6,99)N(I-1),Y
99    FORMAT(' ',2E20.5)
C      FIND JUNCTION DEPTH
      IF(N(I).LT.NB)GO TO 30
5     CONTINUE
C      CALCULATE SHEET RESISTANCE
30    R=RS(CON,N1,RX)
      T3=T3/60.0
      T1=T1/60.
      T2=T2/60.
      T3=T3-T2
      T2=T2-T1
      WRITE(6,20)R,Y,T1,T2,T3,XK,A0

```



```
IF(CN.GT.2.35E20)A=0.456
```

```
5 G = B*(CN**A)
```

```
RETURN
```

```
END
```

```
FUNCTION RS(CON,N,DX)
```

```
DIMENSION CON(N)
```

```
SUM=0.0
```

```
X=0.0
```

```
DO 1 I=1,N
```

```
B=4.0
```

```
IF(1/2*2.E0.I)B=2.0
```

```
IF(1.E0.I)B=1.0
```

```
IF(1.E0.N)B=1.0
```

```
SUM=SUM+CON(I)*B
```

```
1 CONTINUE
```

```
R=DX/3.*SUM
```

```
RS=1./R
```

```
RETURN
```

```
END
```

```
SUBROUTINE TRIDAG(JF,L,A,B,C,D,V)
```

```
DIMENSION A(200),B(200),C(200),D(200),V(200)
```

```
DOUBLE PRECISION BETA(200),GAMMA(200)
```

```
BETA(JF)=B(JF)
```

```
GAMMA(JF)=D(JF)/BETA(JF)
```

```
JFP1=JF+1
```

```

DO 100 I=JFP1,L
BETA(I)=B(I)-A(I)*C(I-1)/BETA(I-1)
100 GAMMA(I)=(D(I)-A(I)*GAMMA(I-1))/BETA(I)
LAST=L-JF
V(L)=GAMMA(L)
DO 200 K=1, LAST
I=L-K
200 V(I)=GAMMA(I)-C(I)*V(I+1)/BETA(I)
RETURN
END

```

```

FUNCTION ERFC(A)
DIMENSION Z(15),w(15)
DOUBLE PRECISION X
REAL Z / .09331, .49269, 1.2156, 2.26994, 3.6672, 5.42533,
*7.5659, 10.12022, 13.13028, 16.6544, 20.77647, 25.62389,
$31.40751, 38.53068, 48.02608/
REAL W / .21823, .34212, .26302, .12642, .40206, .85636,
*.12124, .11167, .64599, .22263, .42274, .39218, .14565
*, .14365, .16005/
SUM=0.
DO 1 I=1,15
X=2(I)+A
SUM=SUM+W(I)*EXP(-X**2+X)
1 CONTINUE
ERFC= SUM*EXP(-A)*2.0/SQRT(5.14159)
RETURN
END

```

APPENDIX IV

EXPLICIT PROGRAM LISTING

```

C   PROGRAM FOR CALCULATING IMPURITY PROFILE, JUNCTION DEPTH,
C   AND SHEET RESISTANCE FOR TWO STEP DIFFUSION IN SILICON
      DIMENSION N(100), NDT(100), CON(100), YP(200), Z(200)
      REAL N, NDT, NO, LA, NB
C   IF PLOT OF N(X) IS DESIRED MAKE THE FIRST CARD OUTPT=2,
C   OTHERWISE MAKE THE CARD OUTPT=0.0
      OUTPT=0.0
      OUTPT=2.0
      IF (OUTPT.LT.1.0) WRITE(6,100)
100  FORMAT(/, 'TE1=PREDEP TEMP. DEG.C., TE2=DRIVE-IN TEMP. DEG.C.', /
* 'RS1=PREDEP SHEET RESISTANCE, RS2=DRIVE-IN SHEET RESISTANCE', /
* 'OHNS' / 'XJ=JUNCTION DEPTH, MICRONS, XO=OXIDE THICKNESS'
* ' IN ANGSTROMS' / 'T(N2)= TIME IN NITROGEN, T(O2) = TIME'
* ' IN OXYGEN' / 'T(H2O) = TIME IN STEAM, ALL IN MINUTES' / /,
*14X, 'TE1', 7X, 'TE2', 7X, 'RS1', 7X, 'RS2', 7X, 'XJ', 6X, 'XO',
*6X, 'T(N2)', 5X, 'T(O2)', 5X, 'T(H2O)' /)
C   NB IS THE BACKGROUND DOPING • PER CC
      NB=1.0E15
C   PREDEP TIME (MIN), TEMP (DEG.C.), DRIVE-IN TEMP (DEG.C.),
C   TIME IN N2 (MIN), O2 (MIN), AND STEAM (MIN)
C   INITIAL VALUES OF DATA

```

C SET ICON.LT.2 FOR A BORON NITRIDE PREDEP

ICON=2

T1=0.0

T2=0.0

T3=0.0

IDAT=1

TI1=17.

TE1=980.

TE2=1050.

RS1=72.

C DATA GENERATION PROGRAM

40 CONTINUE

IF(IDAT.GT.6) GO TO 504

T2=0.0

T3=0.0

T1=T1+20.

IDAT=IDAT+1

GO TO 510

504 IF(IDAT.GT.12) GO TO 506

T1=0.0

T2=T2+20.

T3=0.0

IDAT=IDAT+1

GO TO 510

506 IF(IDAT.GT.18) GO TO 508

T1=0.0

```

      T2=0.0
      T3=T3+20.
      IDAT=IDAT+1
      GO TO 510
508  TE2=TE2+50.
      IF(TE2.GT.1200.) STOP
      IDAT=1
      GO TO 40
510  CONTINUE
C    DIFFUSION CONSTANT CM**2/SEC(BORON GIVEN)
      T=TE1+273.
      COND=0.
      GO TO 200
198  D1=2.*DC
      T=TE2+273.
      COND=2.
      GO TO 200
199  D=DC
      GO TO 13
200  IF(T-1423.) 201,201,202
201  TACT=ALOG(7.84)*1273.*1423./150.
      DOB=0.65E-13*EXP(TACT/1273.)/(3.6)
      GO TO 203
202  TACT=ALOG(6.249)*1423.*1473./50.
      DOB=0.65E-12*EXP(TACT/1473.)
      GO TO 203
203  DC=DOB*EXP(-TACT/T)

```

```

IF(COND.LT.1.) GO TO 198
GO TO 199
13 LA=2.0*SQRT(60.*D1*TI1)
   IF(ICON-2) 14,15,15
14 ALNRS=10.19-1.38E-2*TE1-6.24E-2*TI1+7.E-4*TI1**2
   RS1=EXP(ALNRS)
   QSL=0.0
   QSI=0.0
   CALL FINDNO(RS1,LA,NO)
   GO TO 18
15 CALL FINDNO(RS1,LA,NO)
   QSI=0.0
C   SET QSL=-1.0 IF GLASS INTERLAYER IS REMOVED.
   QSL=3.5E16-0.564*NO*LA
   QSL=-1.0
18 T2=T2+T1
   T3=T3+T2
   T1=T1*0.0
   T2=T2*0.0
   T3=T3*0.0
C   OXIDATION RATE STEAM(CS AND BS) AND O2(CO AND BO)
   CO=0.171*EXP(-23.1E3/(TE2+273.))
   CS=2.37*EXP(-22.7E3/(TE2+273.))
   BO=2.18E-9*EXP(-14.4E3/(TE2+273.))
   BS=0.652E-9*EXP(-8.2E3/(TE2+273.))
C   TOTAL TIME FOR GAUSSIAN ESTIMATION
   TI2=T3

```

```

Q=N0*LA*.564
ALPHA=0.45
C   GAUSSIAN ESTIMATION OF JUNCTION DEPTH
-----
C   DIFFUSION EONS. INTEGRATED OVER REGION OF 2*XJ
XJ=(4.*D*TI2*ALOG(Q/(NB*(3.14*D*TI2)**(.5))))**(.5)
C   NORMALIZING FACTORS
X0=SQRT(D*TI2)
DX=2.*XJ/(200.*X0)
DX=2.*XJ/(100.*X0)
DT=DX**2/(4.)
RT=DT*TI2
RX=DX*X0
R=DT/(DX**2)
M=IFIX(1./DT)
J=IFIX(2.*XJ/(X0*DX))
X=0.
C   INITIALIZATION OF CONCENTRATION
DO 1 I=1,J
N(I)=N0*ERFC(X/LA)
X=X+DX*X0
1 CONTINUE
CSS=5.8E15*(TE2)**(1.595)
QSU=0.564*N0*LA
XQ2=0.0
WRITE(6,300)XJ,D,RX,QSL,QSU,CSS
300 FORMAT(/,6E10.3)
L=2

```



```

21 CONTINUE
   NDT(J)=N(J)

C   BOUNDARY CONDITION AT SI-SI-O2 INTERFACE
   IF(L*RT-T1) 120,120,122
122 IF(L*RT-T2) 124,124,126

C   OXIDATION AND DRIVE-IN WITH STEAM
C   IMPURITY FLUX AT SURFACE ASSUMED CONSTANT UNTIL GLASS IS
C   REMOVED OR TRANSFORMED
126 TIMES=ABS(L*RT-T2)
   XK=BS*((1.+4.*(CS**2)*TIMES/BS+4.*(CS**2)*(XO2**2)/(BS**2)
   **4.*CS*XO2/BS)**(.5)-1.0)/(2.*CS)
   IF(QSL.LT.0.0) GO TO 142
   IF(XK-8.E-6) 140,140,142
140 DXO=0.
   GO TO 160
142 DXO =CS/(1.+4.*(CS**2)*(TIMES)/BS+4.*(CS**2)*(XO2**2)
   */(BS**2)+4.*CS*XO2/BS)**(.5)
   GO TO 160

C   OXIDATION AND DRIVE-IN IN DRY OXYGEN
C   IMPURITY FLUX AT SURFACE ASSUMED CONSTANT UNTIL GLASS
C   LAYER IS TRANSFORMED
124 TIME0=ABS(L*RT-T1)
   XO2=BO*((1.+4.*(CO**2)*TIME0/BO +8.E-6*CO/BO)**(.5)-1.)/
   *(2.*CO)
   IF(QSL.LT.0.0) GO TO 146
   IF(XO2-8.E-6) 144,144,146

```

```

144 DX0=0.0
    GO TO 160

146 DX0 =C0/(1.+4.*(C0**2)*( TIME0 )/B0+8.E-6*C0/B0)**(.5)
    GO TO 160

C    DIFFUSION IN NITROGEN - ACCOUNTS FOR BORON GLASS NOT
C    REMOVED FROM THE SURFACE BY THE HF ETCH

120 IF(QSL.LT.0.0) GO TO 152
    IF(QSI-QSL) 150,150,152

150 F=D*(CSS-N(2))/RX
    DQSI=F*RT
    QSI=QSI+DQSI
    DX0=0.0
    GO TO 162

152 F=0.0
    DX0=0.0
    GO TO 162

160 F=(ALPHA-3.33)*DX0*N(1)

162 GA=0.45*RT/RX*DX0
    JO=J-1

C    THIS IS AN ARTIFICIAL BOUNDARY CONDITION TO MAKE N(X)
C    FINITE AT 2*XJ AND EQUAL TO GAUSSIAN VALUE
    IF(L.GT.10)NDT(J)=Q/(1.79*SQRT(D*L*RT))*EXP(-(J*RX)**2)/
    *(4.*D*L*RT)

C    INTEGRATION OF NORMALIZED DIFFUSION EQUATIONS
    DO 2 I=2,JO
    NDT(I)=R*N(I+1)+(1.-2.*R+GA)*N(I)+(R-GA)*N(I-1)
    IF(NDT(I).LT.1.0E-15)NDT(I)=1.0E-15

```

```

2 CONTINUE
  IF(N(1)+(DX*X0*F)/D.LT.0.)F=-NDT(2)*D/(RX)
  NDT(1)=DX*F*X0/D+NDT(2)
  DO 3 I=1,J
  N(I)=NDT(I)
3 CONTINUE
  IF(L.GE.M) GO TO 6
  L=L+1
  GO TO 21
4 CONTINUE
6 CONTINUE
  K=2
  DO 5 I=2,J
C   MAKE NEXT INSTRUCTION CARD , C=N(I-1) FOR P-TYPE
C   MAKE NEXT INSTRUCTION CARD ,C=-N(I-1) FOR N-TYPE
  C=N(I-1)
C   G(C) USES IRWIN'S CURVE FORMULAS
  CON(I-1)=G(C)
  N1=I-1
  Y=I*RX-2.*RX
  YP(K)=Q*EXP(-(P*RX)**2/(4.*D*TI2))/SQRT(3.14*D*TI2)
  YP(K-1)=N(I-1)
  Z(K-1)=I*RX
  P=N1
  YP(1)=YP(2)
  Z(K)=Z(K-1)
  K=K+2

```

```

      IF(N(I-1).LT.NB.AND.N(I).LT.N(I-1))GO TO 30
5  CONTINUE
C  INTEGRATION FOR RS,SHEET RESISTANCE
-----
30  RS2=RS(CONFNI/RX)
      IF(OUTPT.GT.1.0) CALL PLOT(Z,YP,K-2,NB,Y)
      XK=BS*((1.+4.*(CS**2)*(T3-T2)/BS+4.*(CS**2)*(X02**2)/
* (BS**2)+4.*CS*X02/BS)**(.5)-1.0)/(2.*CS)
      T1=T1/60.
      T2=T2/60.
      T3=T3/60.0
      T3=T3-T2
      T2=T2-T1
      IF(OUTPT.GT.1.0) WRITE(6,20) RS2 Y,T1,T2,T3,XK,TE2
20  FORMAT(/,10X,'SHEET RESISTANCE= ',F8.2//,10X,'JUNCTION'
*' DEPTH IN CM=' ,E10.3//,10X,'TIME IN NITROGEN IN '
*' MINUTES = ',F9.1//,10X,'TIME IN OXYGEN IN '
*' MINUTES = ',F9.1//,10X,'TIME IN STEAM IN MINUTES = ',
*F9.1//,10X,'OXIDE THICKNESS IN CM = ',E10.2//,
*10X,'DRIVE-IN DIFFUSION TEMP IN DEG. C. = ',F9.1)
      XKA=1.E8*XK
      YM=1.E4*Y
      IF(OUTPT.LT.1.0) WRITE(6,22)TE1,TE2,RS1,RS2,YM,XKA,T1,T2,T3
22  FORMAT(/,10X,9F10.3)
400 CONTINUE
      GO TO 40
      END

```

SUBROUTINE FINDNO(RS1,LA,NO)

C FINDNO IS BASED ON THE RELATION SHIP FOR RS FOR AN ERFC
C PROFILE. IT WAS CALCULATED FROM A NUMERICAL
C INTEGRATION, AND THEN FITTED WITH A PIECEWISE
C CONTINUOUS FUNCTION.

REAL NO,LA

GAVE=1.0/(RS1*LA)

ALPA=.3E-10

ALPB=.628E-14

ALPC=.369E-16

BETA=0.646

BETB=0.842

BETC=0.956

IF(GAVE<155.) 4,6,6

4 IF(GAVE<40.) GO TO 8

ALOGC=ALOG(GAVE/ALPB)/BETB

GO TO 10

6 ALOGC=ALOG(GAVE/ALPC)/BETC

GO TO 10

8 ALOGC=ALOG(GAVE/ALPA)/BETA

GO TO 10

10 NO=EXP(ALOGC)

RETURN

END

REAL FUNCTION ERFC(U)

IF(U<1.0) 3,5,5

```

3  N=31
   GO TO 15
5  IF(U-2.0) 7,9,9
-----
7  N=41
   GO TO 15
9  IF(U-2.5) 11,13,13
11 N=61
   GO TO 15
13 IF(EXP(-U**2).LT.1.E-15)ERFC=1.E-15
    IF(EXP(-U**2).LT.1.E-15)RETURN
    ERFC=EXP(U.-U**2)/(1.772*U)
    GO TO 17
15 SU=0.0
    DX=U/(N-1)
    X=0.0
    I=1
1  B=2.0
    IF(I/2* 2.EQ.I)B=4.0
    IF(I.EQ.1) B=1.0
    IF(I.EQ.N) B=1.0
    ER= EXP(0.-X**2)
    SU= SU+ER*B
    X=X +DX
    I=I+1
    IF(N-I) 2,1,1
2  CONTINUE
   S=DX/3.0*SU

```

```

ERFC =1.0 -2.0*5/1.772
17 CONTINUE
RETURN
END

REAL FUNCTION G(CX)
CN= ABS(CX)
IF(CX.LT.0.0) GO TO 3
IF(CN.GT.0.0) A=1.0
IF(CN.GT.0.0) B=7.2E-17
IF(CN.GT.1.5E +16) A=0.65
IF(CN.GT.1.5E +16)B=3.3E-11
IF(CN.GT.2.4E+18) A=0.832
IF(CN.GT.2.4E+18)B=1.47E-14
IF(CN.GT.1.5E+19) A=0.966
IF(CN.GT.1.5E+19)B=4.E-17
GO TO 5
3 IF(CN.GT.0.0) A=1.0
IF(CN.GT.0.0)B=2.E-16
IF(CN.GT.3.5E15)A=0.837
IF(CN.GT.3.5E15)B=6.97E-14
IF(CN.GT.1.0E17) A=0.543
IF(CN.GT.1.0E17)B=6.93E-9
IF(CN.GT.9.5E18) A=0.94
IF(CN.GT.9.5E18)B=2.E-16
IF(CN.GT.6. E19) A=0.744
IF(CN.GT.6. E19)B=1.43E-12

```

```
IF (CN.GT.2.35E20)A=0.456
IF (CN.GT.2.35E20) B=1.04E-6
```

```
5 6 = B*(CN**A)
```

```
RETURN
END
```

```
FUNCTION RS(CON,N,DX)
```

```
DIMENSION CON(N)
```

```
SUM=0.0
```

```
X=0.0
```

```
DO 1 I=1,N
```

```
B=2.0
```

```
IF (I/2+2.EQ.I)B=4.0
```

```
IF (I.EQ.1)B=1.0
```

```
IF (I.EQ.N)B=1.0
```

```
SUM=SUM+CON(I)*B
```

```
1 CONTINUE
```

```
R=DX/3.*SUM
```

```
RS=1./R
```

```
RETURN
```

```
END
```

```
SUBROUTINE PLOT(X1,Y1,N,NB,XJ)
```

```
REAL NB
```

```
DIMENSION X1(250),Y1(250),ARRAY(45,101)
```

```
DATA AST,DASH,BAR,BLANK/1H*,1H-,1H],1H /
```

```
DO 19 L=1,45
```



```

DO 19 M=1,101
  ARRAY(L,M)= BLANK
19 CONTINUE
  DO 20 M=1,101
    ARRAY(1,M)=DASH
    ARRAY(45,M)=DASH
20 CONTINUE
  DO 22 L=1,45
    ARRAY(L,1)=BAR
    ARRAY(L,101)=BAR
22 CONTINUE
  CMAX=ABS(Y1(1)-NB)
  CMIN=ABS(Y1(1)-NB)
  XMAX=X1(N)
  DO 4 I=2,N
    Z1=ABS(Y1(I)-NB)
    IF(Z1.GT.CMAX) CMAX=Z1
    IF(Z1.LT.CMIN) GO TO 12
  GO TO 14
12 CMIN=Z1
  GO TO 14
14 IF(Z1.LT.1.0) Z1=1.0
  Z2=ALOG10(Z1)
  L=(85.-4.*Z2)
  M=(101.*(X1(I))/XMAX+.5)
  IF(L.LT.1) L=1
  IF(L.GT.45) L=45

```

```

IF(M.LT.1) M=1
IF(M.GT.101) M=101
ARRAY(L,M)=AST
-----
4  CONTINUE
   XJM=1.E4*XJ
   WRITE(6,30) CMAX,CMIN,XJM
30  FORMAT(1H1,10X,'CMAX= ',E8.3,5X,'CMIN= ',E8.3,5X,
* 'XJ(MICRONS)=',F6.3/)
   L=1
   WRITE(6,80) (ARRAY(L,M), M=1,101)
80  FORMAT(' ',10H-----,101A1)
   L=2
   WRITE(6,82) (ARRAY(L,M),M=1,101)
82  FORMAT(' ',1HJ,' C(X) ',101A1)
   L=3
   WRITE(6,84) (ARRAY(L,M),M=1,101)
84  FORMAT(' ',1HJ,9X,101A1)
   L=4
   WRITE(6,86) (ARRAY(L,M),M=1,101)
86  FORMAT(' ',1HJ,' PER CC ',101A1)
   IT=1
   DO 32 L=5,45
   EX=10.**((L-1)/4)
   CX=1.E21/EX
   IF((L-1).EQ.(4*IT)) GO TO 40
   WRITE(6,88) (ARRAY(L,M),M=1,101)
88  FORMAT(' ',1HJ,9X,101A1)

```

```

GO TO 32
40 WRITE(6,90) CX,(ARRAY(L,M),M=1,101)
90 FORMAT(' ',2HJ ,E6.1,2H--,101A1)
    IT=IT+1
32 CONTINUE
    WRITE(6,94)
94 FORMAT(' ',1HJ,9X,1HJ,9X,1HJ,9X,1HJ,9X,1HJ,9X,1HJ,9X,1HJ,9X,
*1HJ,9X,1HJ,9X,1HJ,9X,1HJ,9X)
    XAA=2.E3*XMAX
    XAB=4.E3*XMAX
    XAC=6.E3*XMAX
    XAD=8.E3*XMAX
    XAE=1.E4*XMAX
    WRITE(6,96) XAA,XAB,XAC,XAD,XAE
96 FORMAT(/ ,10X,1H0,17X,F5.2,15X,F5.2,15X,F5.2,15X,F5.2,
*15X,F5.2)
    WRITE(6,98)
98 FORMAT( /,45X,'X -MICRONS')
    RETURN
    END

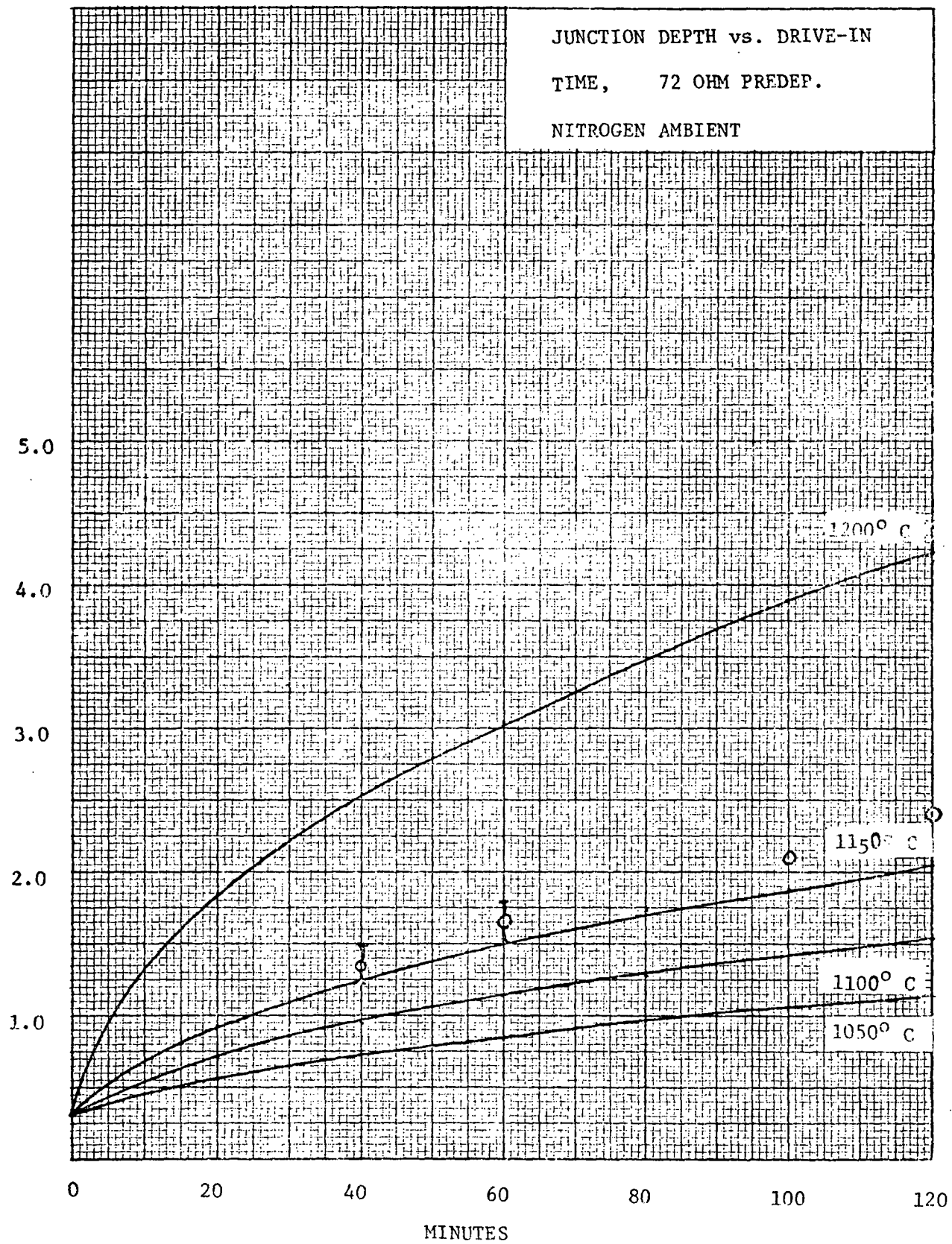
```

APPENDIX V

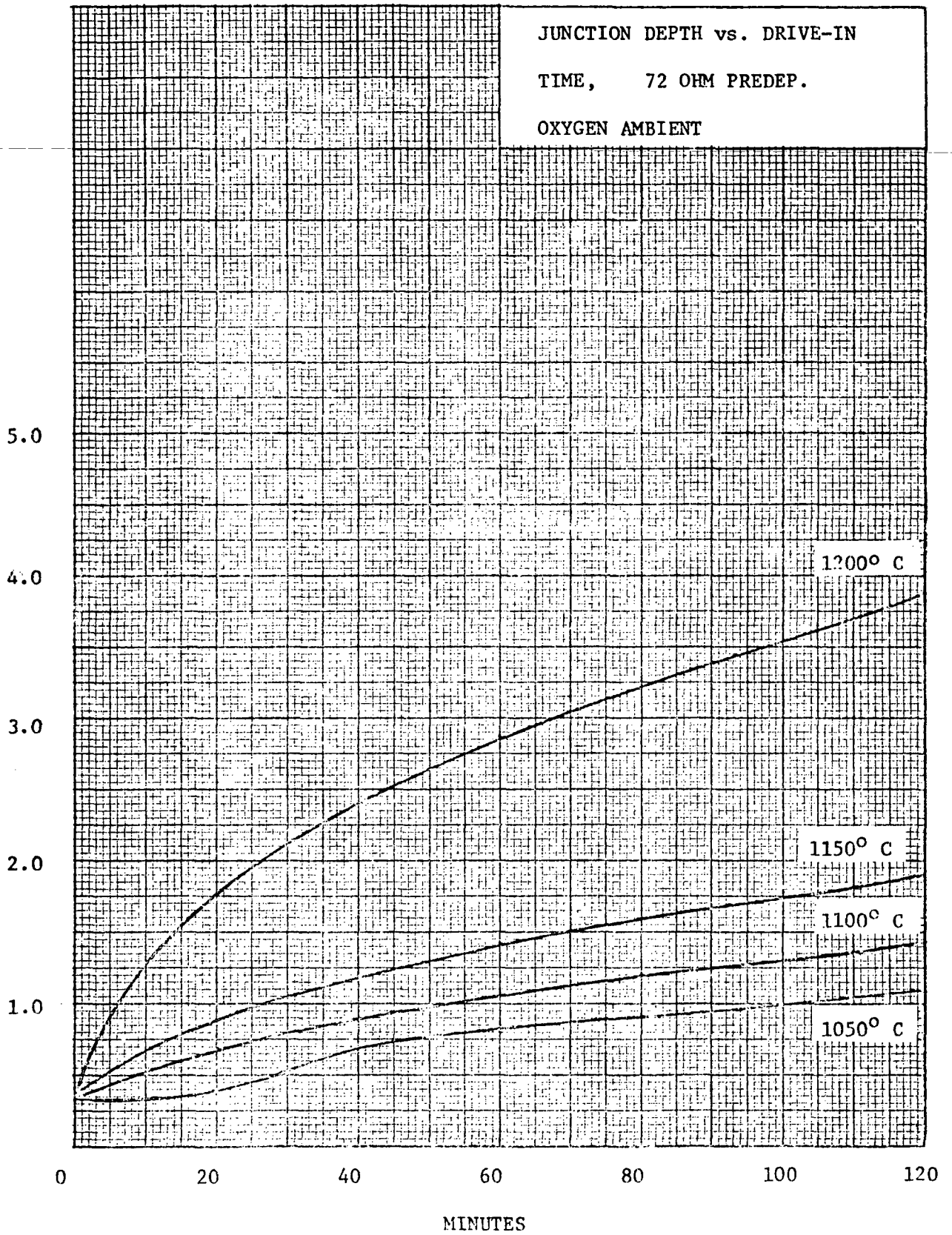
JUNCTION DEPTH, SHEET RESISTANCE, and OXIDE THICKNESS CURVES

The curves given in this appendix are for drive-in diffusions in nitrogen, oxygen, and steam at drive-in temperatures of 1050°C, 1100°C, 1150°C, and 1200°C. The predeposition diffusions are assumed to be the 72 ohm or 27 ohm diffusions carried out at 980°C that are done at MSFC. The 72 ohm prep is for 17 minutes in diborane followed by 7 minutes in O₂. The 27 ohm prep is for 60 minutes in diborane followed by 6 minutes in N₂. All the boron glass is assumed to be removed for the 72 ohm diffusion, but the boron-rich interlayer is assumed to remain for the 27 ohm diffusion. The explicit integration program listed in Appendix IV was used to generate the data. Experimental data is given on graph V-5 which has some scatter in the resistance after predeposition. All experimental data points are for 1150°C diffusion and are shown as circles with data spread indicated by a vertical bar.

MICRONS

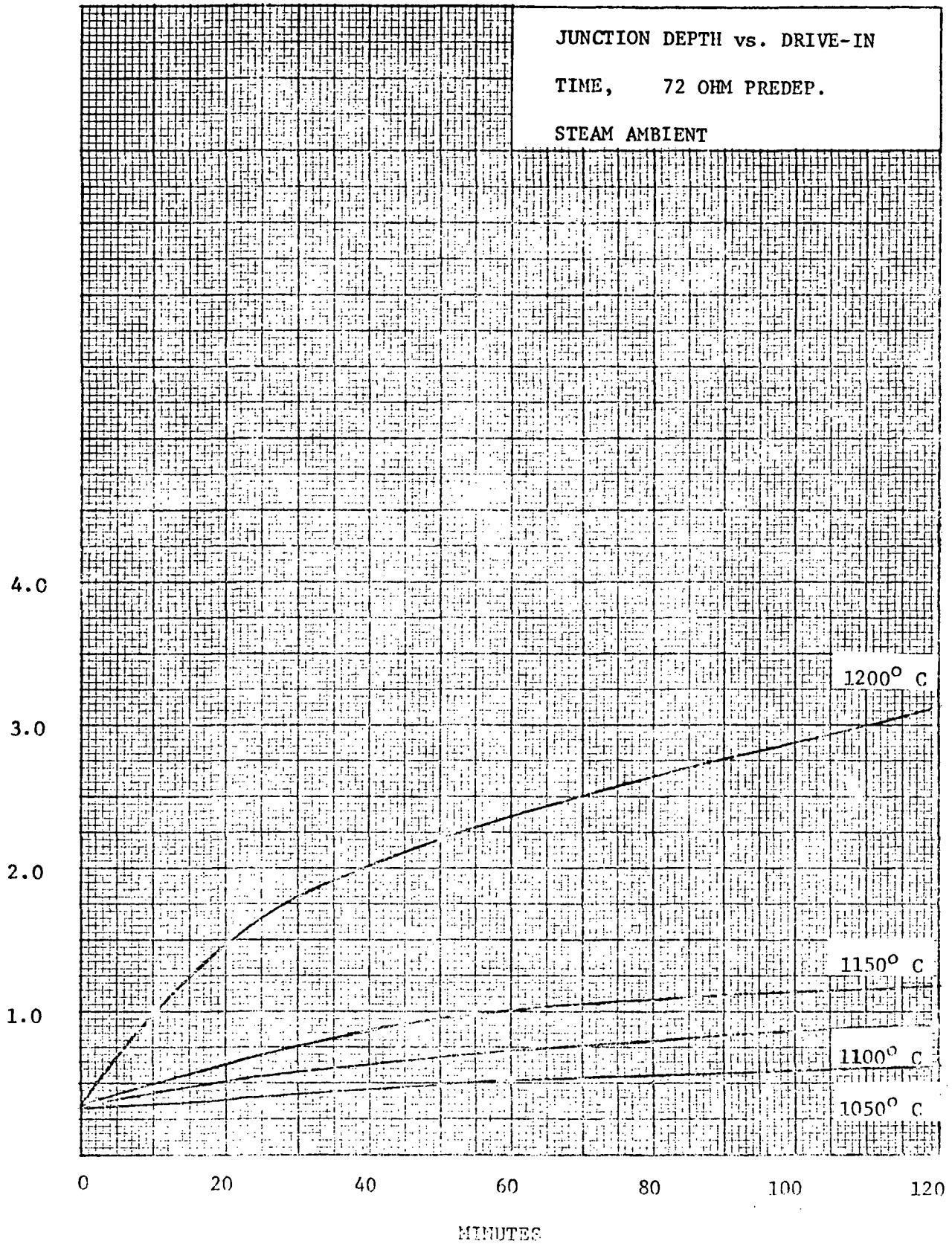


MICRONS



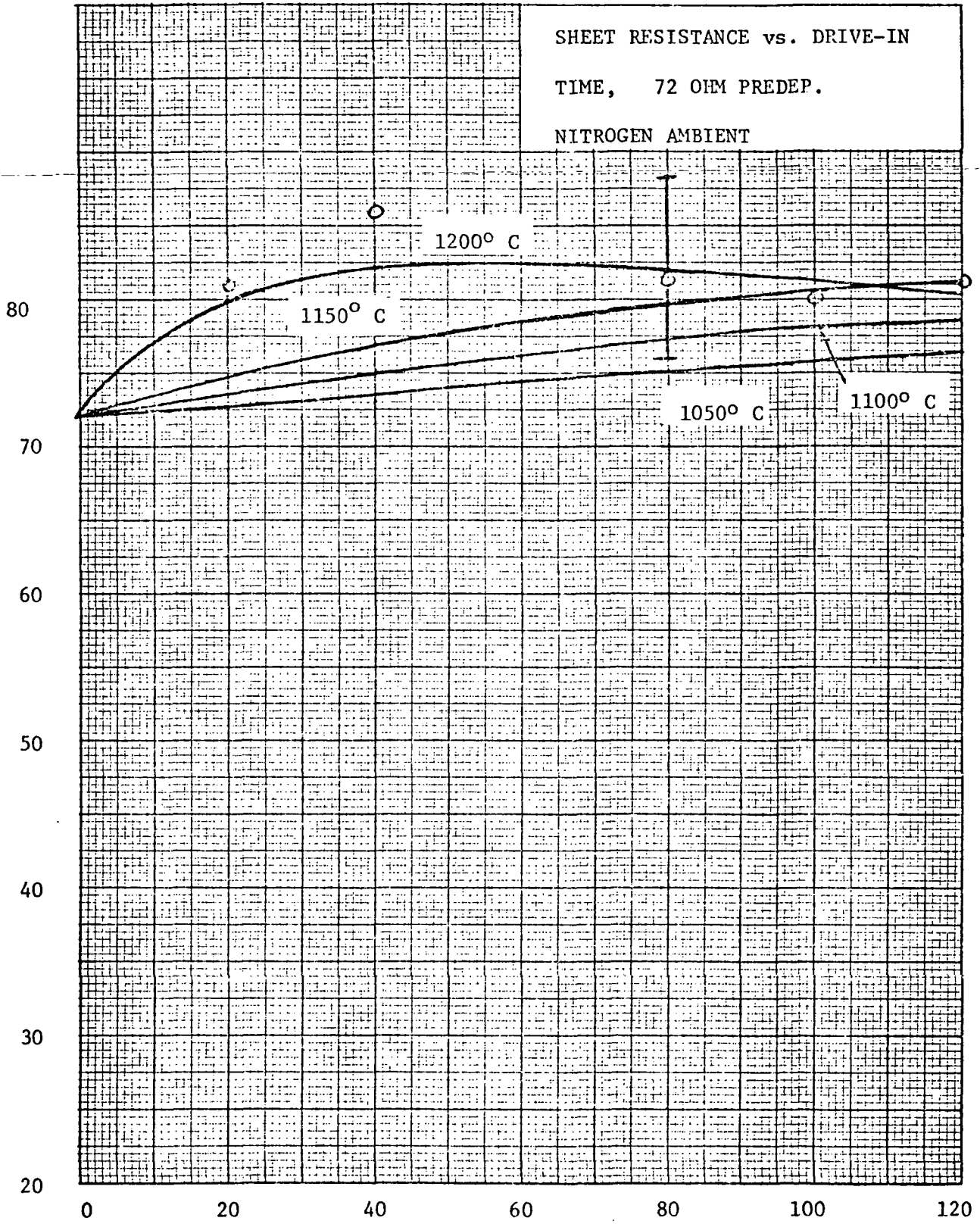
MICRONS

JUNCTION DEPTH vs. DRIVE-IN
TIME, 72 OHM PREDEP.
STEAM AMBIENT



MINUTES

OHMS

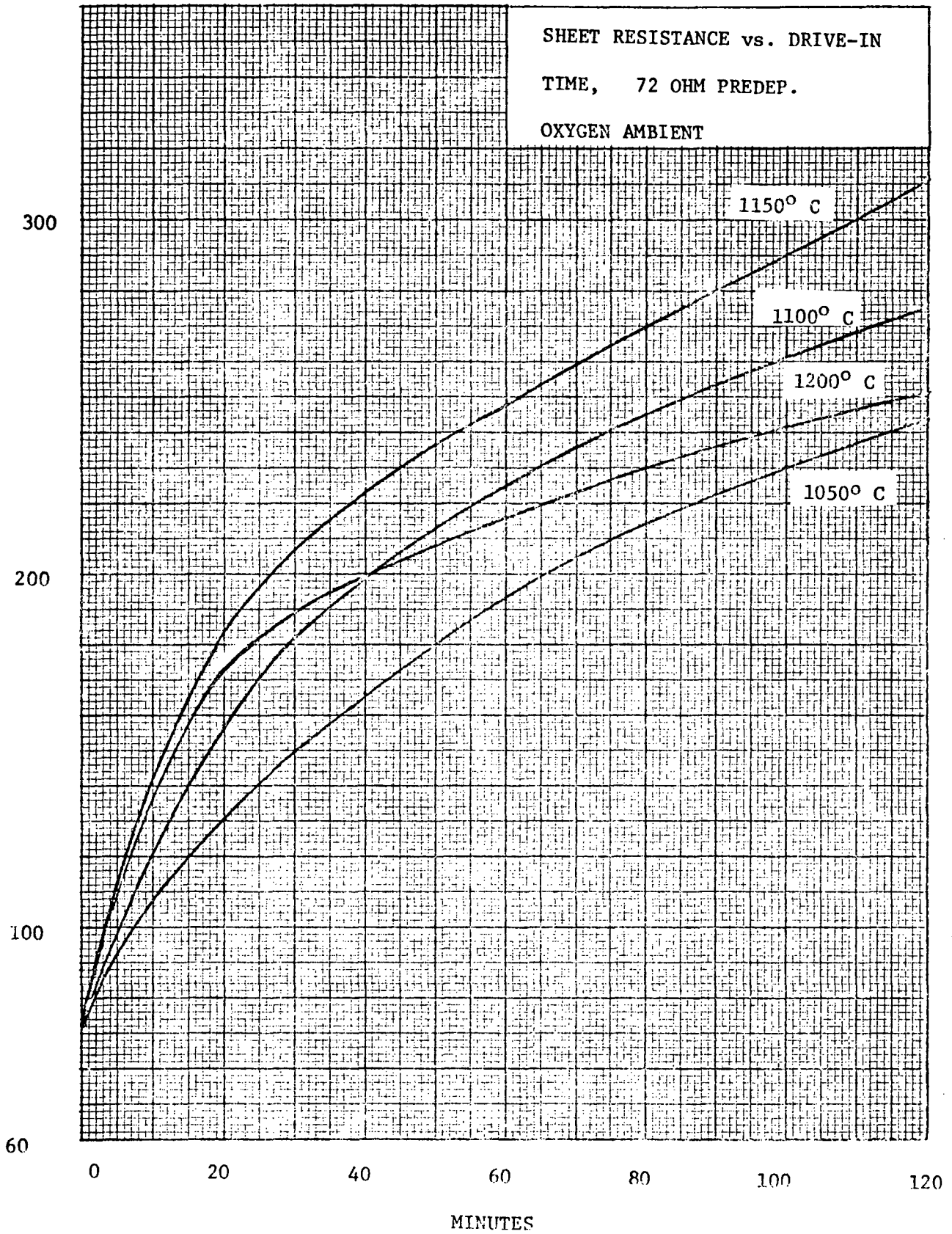


SHEET RESISTANCE vs. DRIVE-IN
TIME, 72 OHM PREDEP.
NITROGEN AMBIENT

Experimental points are shown for 1150° C drive-in.
Predep. resistance was between 69 and 77 ohms.
MINUTES V-5

OHMS

SHEET RESISTANCE vs. DRIVE-IN
TIME, 72 OHM PREDEP.
OXYGEN AMBIENT



OHMS

SHEET RESISTANCE vs. DRIVE-IN
TIME, 72 OHM PREDEP.
STEAM AMBIENT

6000

5000

4000

3000

2000

1000

0

20

40

60

80

100

120

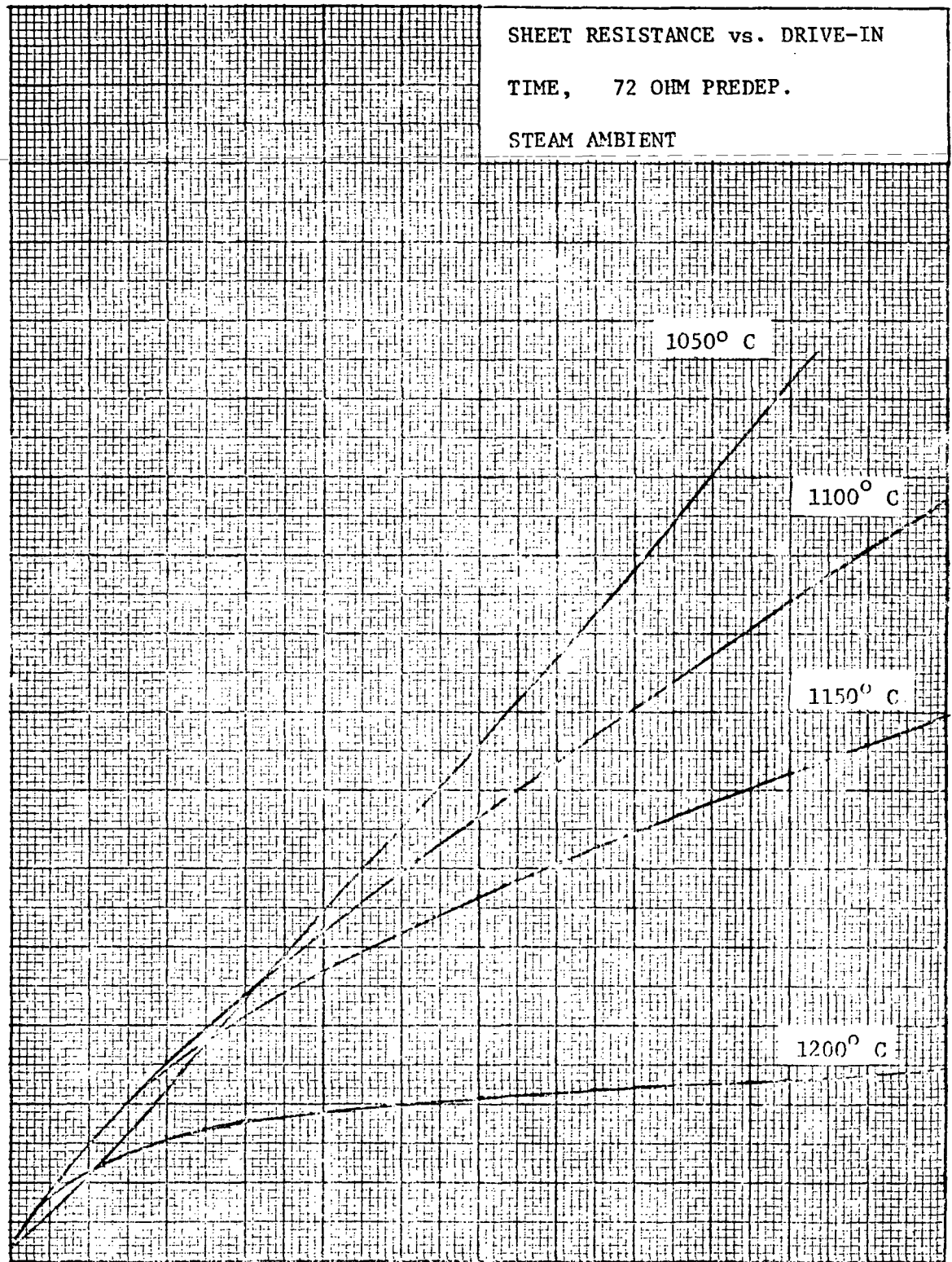
MINUTES

1050° C

1100° C

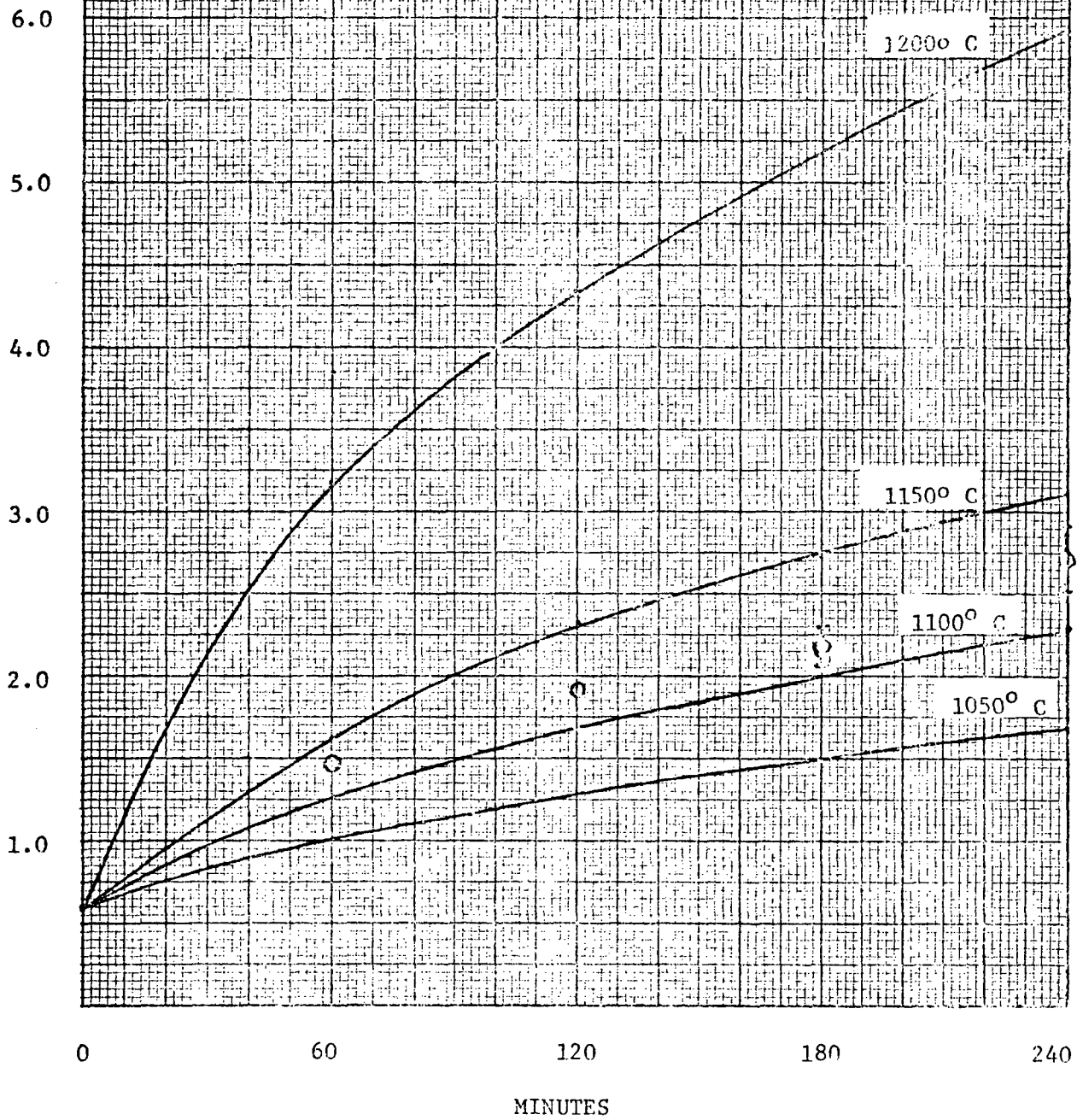
1150° C

1200° C



MICRONS

JUNCTION DEPTH vs. DRIVE-IN
TIME, 27 OHM PREDEP.
NITROGEN AMBIENT



MICRONS

JUNCTION DEPTH vs. DRIVE-IN

TIME, 27 OHM PREDEP.

OXYGEN AMBIENT

6.0

5.0

4.0

3.0

2.0

1.0

1200° C

1150° C

1100° C

1050° C

0

60

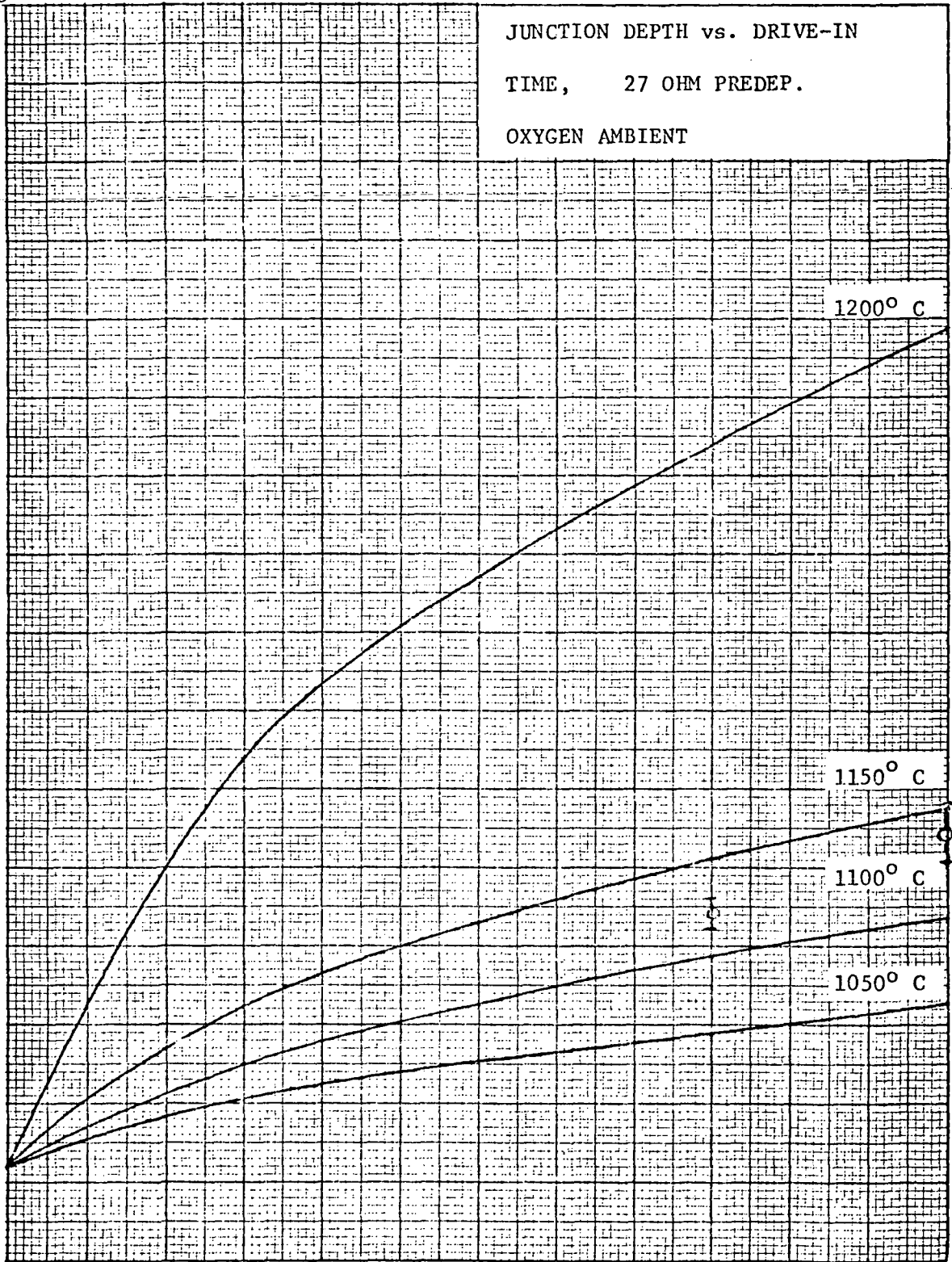
120

180

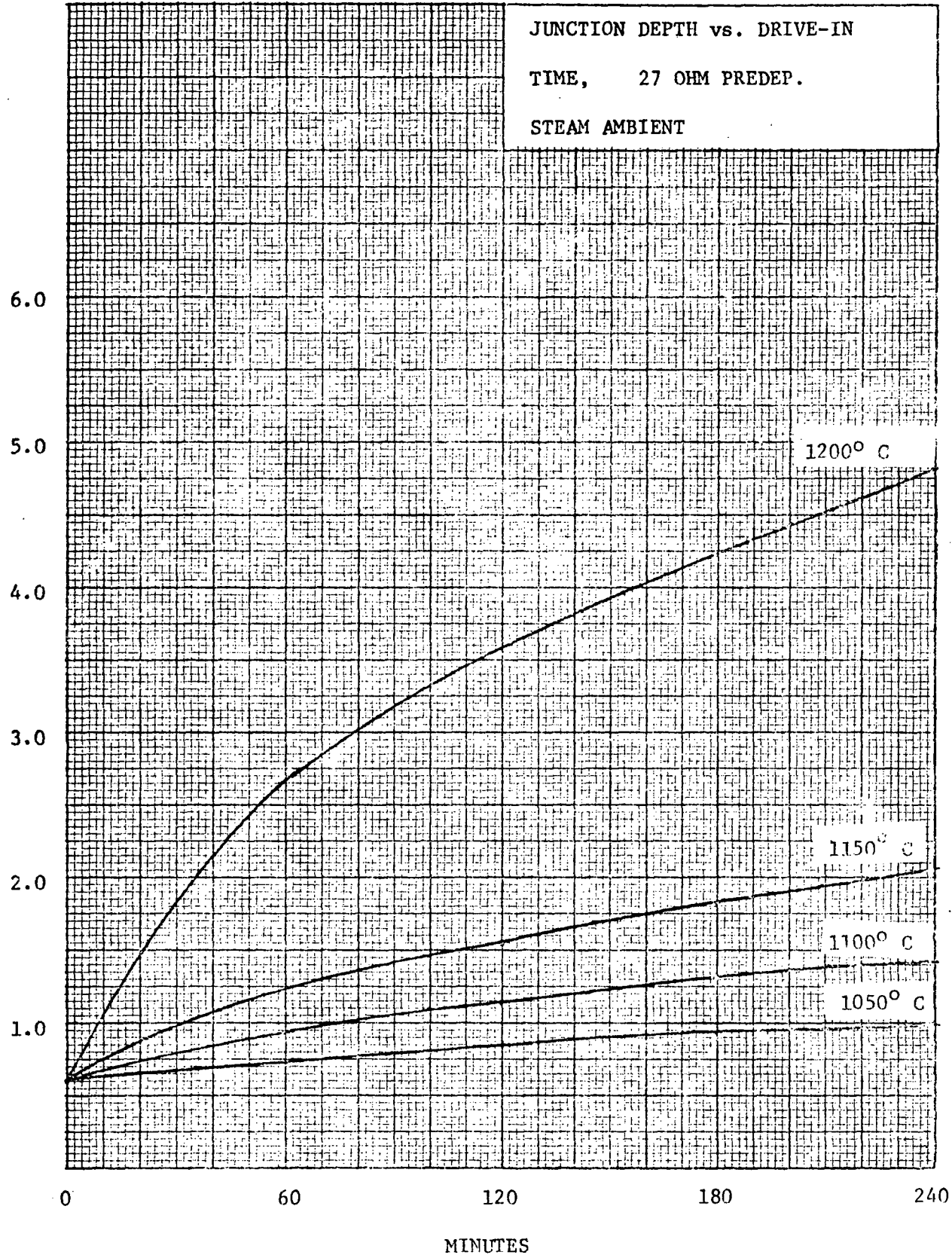
240

MINUTES

V-9



MICRONS



OHMS

30

25

20

15

10

5

SHEET RESISTANCE vs. DRIVE-IN

TIME, 27 OHM PREDEP.

NITROGEN AMBIENT

1050° C

1100° C

1150° C

1200° C

0

60

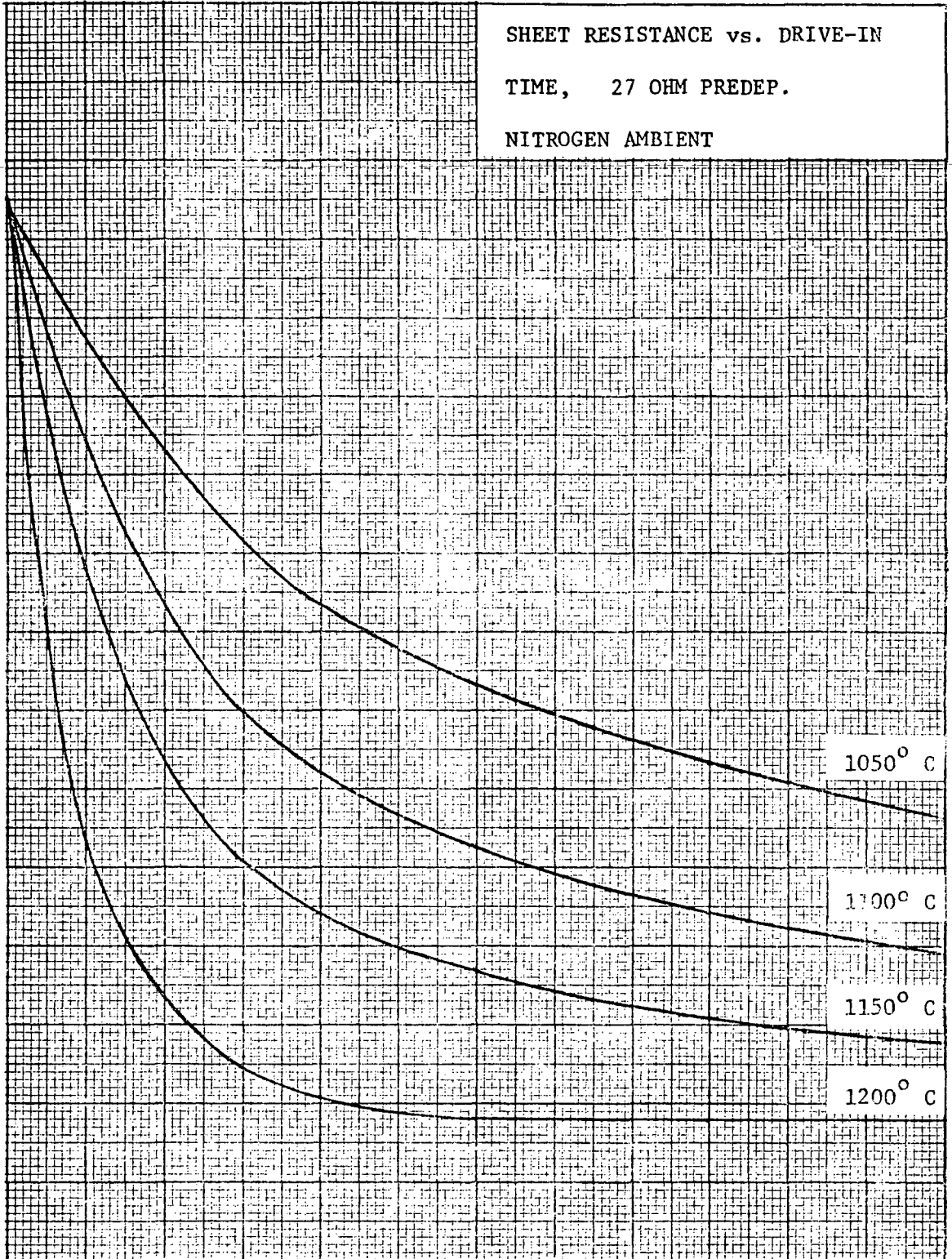
120

180

240

MINUTES

V-11

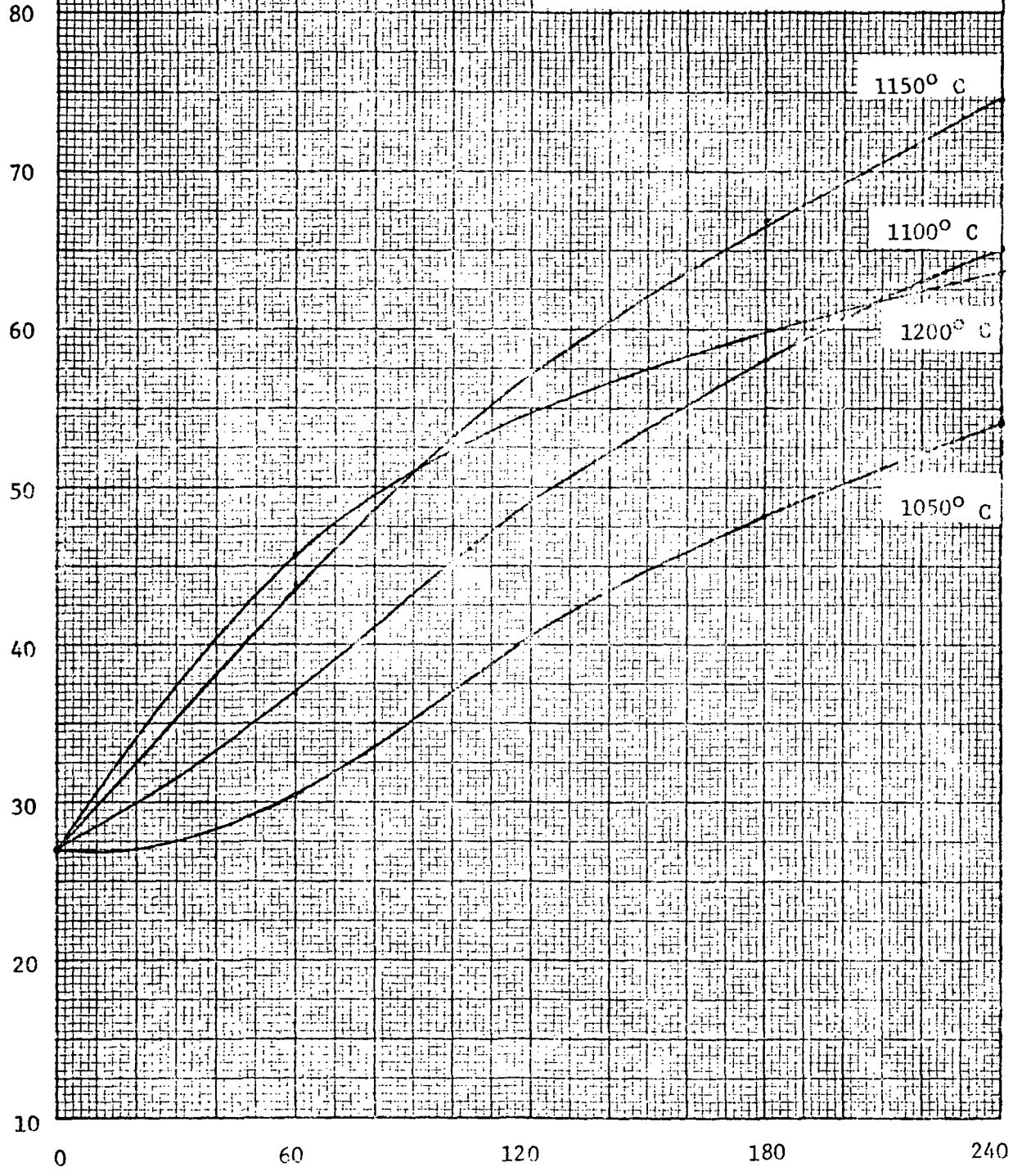


OHMS

SHEET RESISTANCE vs. DRIVE-IN

TIME, 27 OHM PREDEP.

OXYGEN AMBIENT



MINUTES

OHMS

SHEET RESISTANCE vs. DRIVE-IN
TIME, 27 OHM PREDEP.
STEAM AMBIENT

1400

1050° C

1200

1100° C

1000

1150° C

800

600

400

1200° C

200

0

60

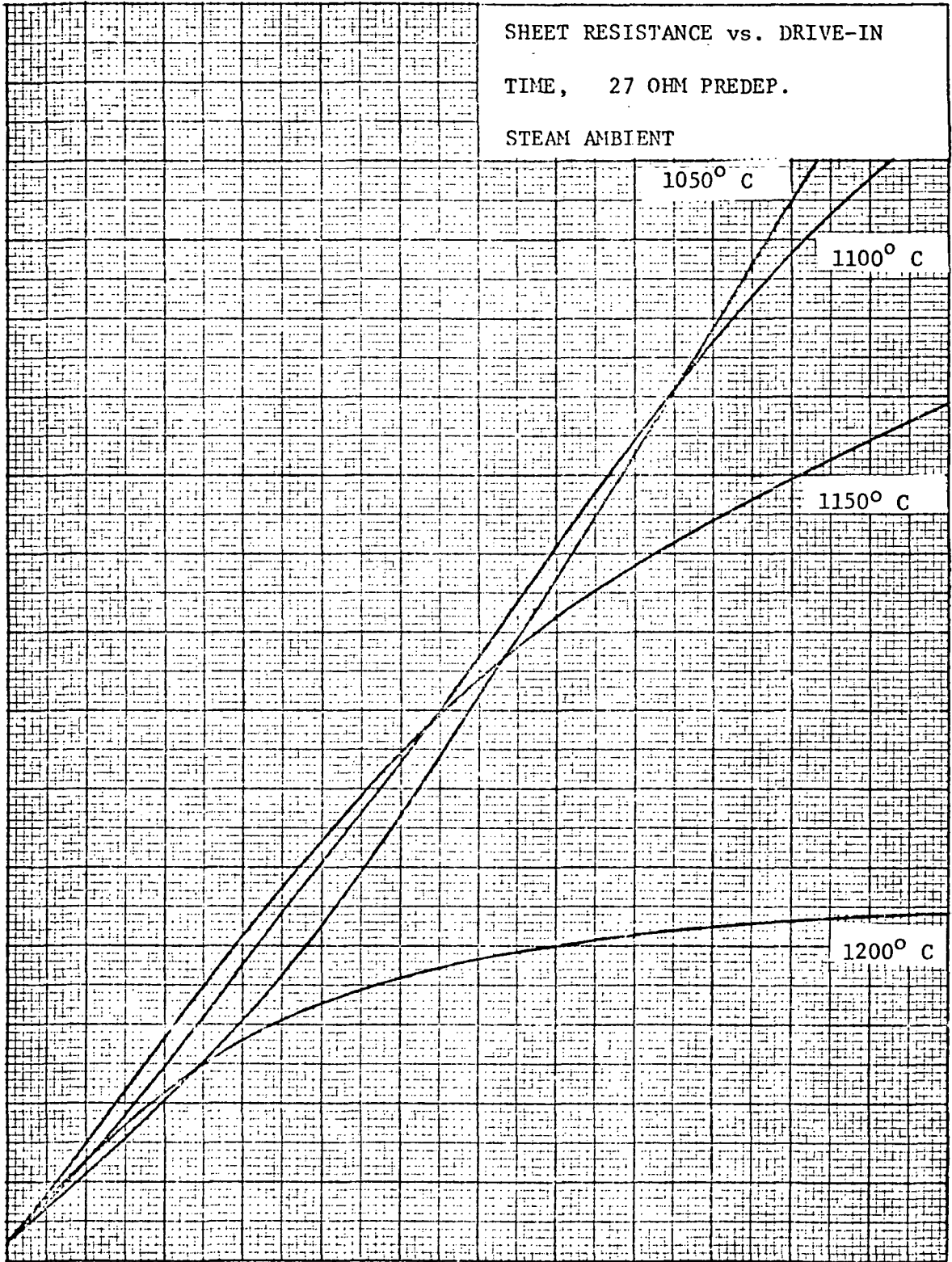
120

180

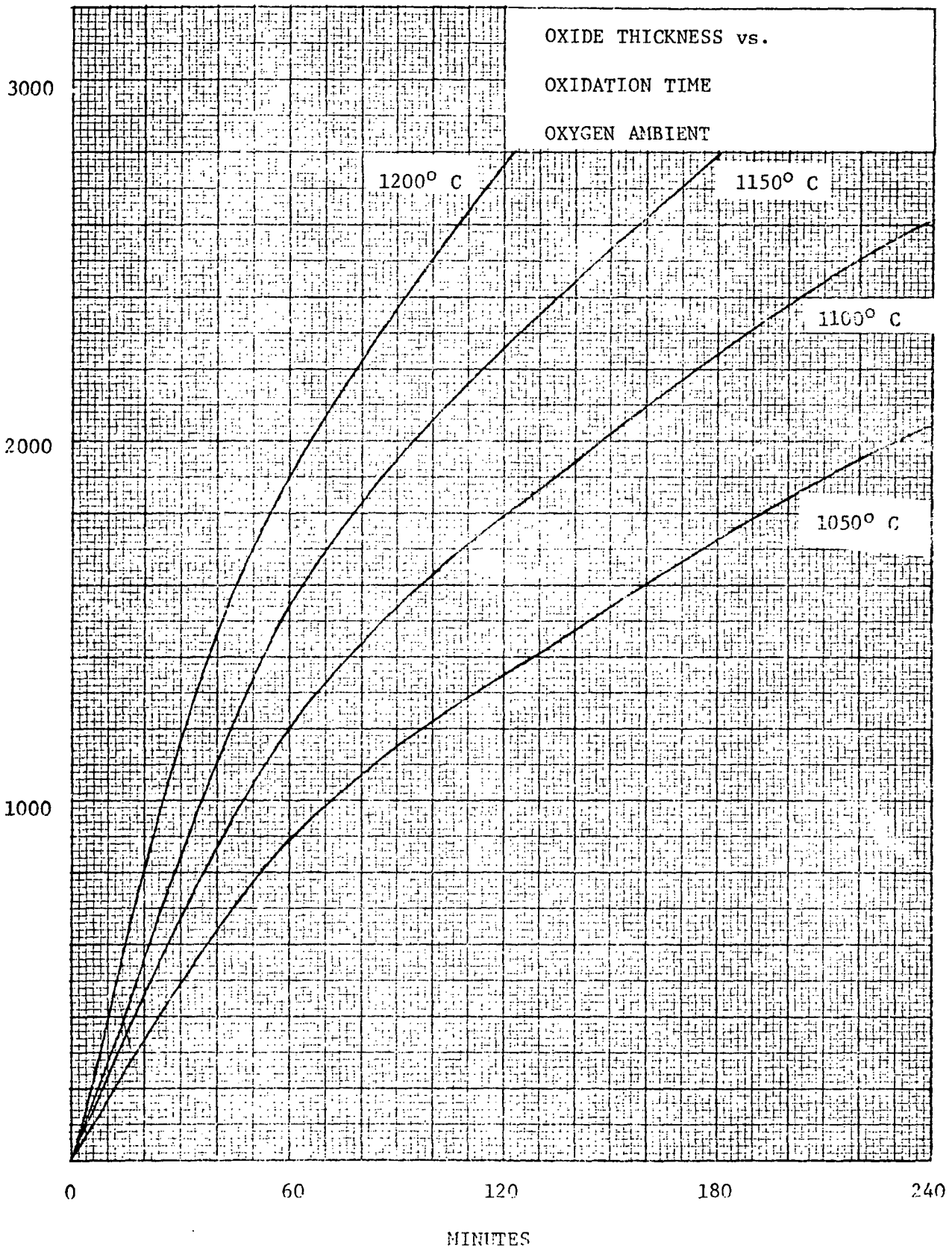
240

MINUTES

V-13



ANGSTROMS



V-14